IMU Validation Apparatus for Human Joints

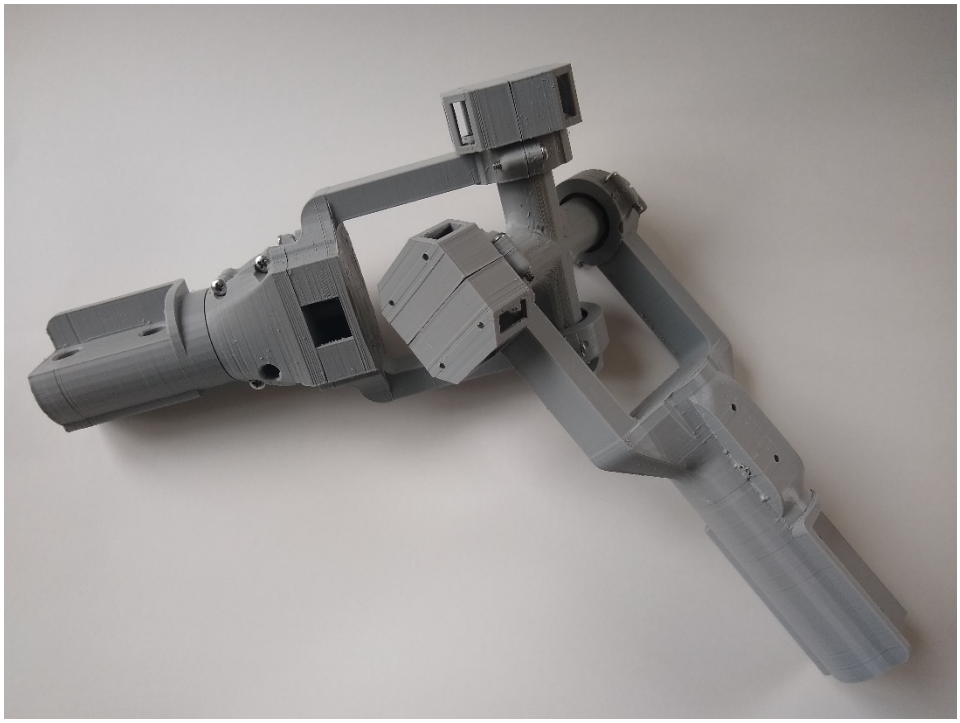

Final Report

Isaac Harris, Chelsea Nienhuis, Alex Rees, Ziqi Wang, Keyen Yockey

University of Michigan - Department of Mechanical Engineering

ME 450 - Fall 2020 - Team 22

Sponsor: Dr. Stephen Cain

Mentor: Dr. Noel Perkins

December 08, 2020

TABLE OF CONTENTS

Executive Summary

Our ME450 team is made up of five mechanical engineering students. This course is an opportunity for us to go through an industry-like process to create a new device or procedure for a stakeholder.

Inertial measurement units (IMUs) are small sensors packs that include accelerometers, gyroscopes, and magnetometers that are used to conduct movement analysis outside of a laboratory setting. IMUs use an integration process to output data that can be used to determine absolute orientation and location of the object they are attached to, so error in their output is vulnerable to discrepancies from the effects of long-term data collection. To combat this, post-processing algorithms can be made to adjust for these measurement errors. Our stakeholder, Dr. Stephen Cain, and his lab have written algorithms that they believe should account for this measurement error; however, they need a way to record ground-truth data to compare their results with. Our task for our ME450 Capstone Project is to design an apparatus that can independently measure orientation between two end links while simultaneously allowing for IMU measurements of the orientations in order to validate the IMU algorithms.

Based on our discussions with Dr. Cain and our background research, we constructed requirements and specifications for our project. Twelve requirements, broken up into three tiers based on their relative importance, have been identified to define the needs for our validation instrument. Each requirement has at least one technical specification corresponding to it that quantifies the desired attribute(s) given in the requirement. Our requirements and specifications are shown in Table 4 on pages 9-10.

Our team then moved into a concept evaluation phase, where we generated large quantities of ideas on how to design the IMU validation apparatus. For this concept evaluation process, we broke our problem up into the following eight categories: angular sensor, joint design, degree of freedom locking, end-link material, end-link features, data acquisition, rigid body connection, and IMU connection. For each of these categories, the top solutions were selected by determining the generated idea's ability to fulfill our requirements and specifications.

In the solution development phase, we built on our concept evaluation process and settled on the final design for our project. Our final design consists of a universal joint and a pivot joint with capacitive sensors for measuring angles. Our choices were based off of our apparatus' ability to measure angles within our specified error range, ability to achieve a range of motion of 180 degrees around each axis, and its portability. A full CAD model was developed based on our selected components, and a bill of materials was created based off of the model.

Lastly, we proceeded into the verification phase of the project. During this phase, we determined verification tests that would allow use to test the validity of our solution. To do this, we created a first-iteration prototype that underwent some of the testing methods that we'd outlined. Due to time constraints, we were unable to complete all of our testing; however, we were able to conduct Failure Modes and Effects Analysis (FMEA) that provides solutions for a variety of failures that our device could undergo beyond the scope of the testing we were able to complete. Our goal is to present our stakeholder, Dr. Cain, with a physical prototype that achieves basic functionality before the end of the 2020 calendar year.

Background and Problem Description

The project's focus on IMUs is motivated by the limitations of the current state of the art human motion capture (MOCAP) systems. These MOCAP setups consist of a collection of cameras that record movements by tracking reflective markers attached to key landmarks on body segments. While the markers are lightweight and allow for accurate motion tracking of the entire body, these types of systems are expensive and constrain the researcher or end user to a laboratory setting only [1], [2].

Despite researcher's best efforts, it is difficult to recreate natural human activity within a controlled lab environment. First and foremost, the physical size of the lab building and the measurement volume of the camera system significantly limits the space in which movement can be performed [1]. When examining simple lower limb joint kinematics, the size constraint is often avoided by placing the subject on a treadmill in the center of the motion capture volume, however it has been shown that belt dynamics can often induce unnatural joint kinematics [3]. Additionally, the treadmill solution does nothing to accommodate activities other than linear walking and running. Second, many researchers are interested in analyzing how joint kinematics change with fatigue [4]. Depending on the study, this could mean analyzing the subject over an entire day or week, far longer than a single trial in the lab could accommodate. Third, when subjects (especially children) are studied in a lab setting they often alter their kinematics in order to "perform" for the researcher, producing results counter to their natural movement [5]. There are many applications in which the ability to track human motion outside the lab would be useful but are not feasible in a laboratory. For example, a physical therapist often provides a limited number of in person training sessions for patients, and then proceeds to send the patient home with exercises they should perform on their own. In this circumstance, the patient-therapist feedback loop could be significantly improved from a device capable of measuring kinematics during at home exercises [6]. Other examples include capturing joint kinematics of someone traversing the uneven terrain of a hiking trail to later be programmed into a robotic prosthesis or analyzing the motion of a basketball player's 3-point shot to help improve their shooting percentage. The list of possibilities when untethered to a laboratory is endless.

With rapid advances in micro-electro-mechanical systems during the 21st century, researchers have looked to inertial measurement units (IMUs) to help conduct experiments outside the lab. These compact devices include a variety of sensors including accelerometers, gyroscopes and magnetometers. Numerous algorithms and experimental setups have been introduced to take advantage of this convenient package of sensors in the context of human motion tracking with varying degrees of success [7]–[12]. Nearly the size of a quarter, their small form factor and low cost make IMUs an appealing alternative to traditional camera systems both inside the lab and out [12, Fig. 1][2]. However, due to various sensor limitations, creating IMU algorithms to measure joint angles with high accuracy is a non-trivial task.

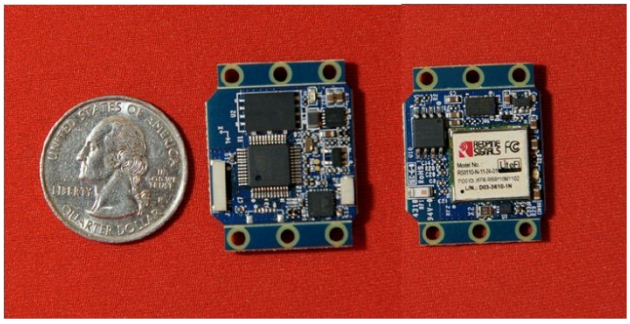

Fig. 1. Miniature IMU nearly the size of a quarter [13]

Estimates of joint angles follow from IMU data by tracking the absolute orientations of two jointed body sections and the direction of the joint axes and combining this information to yield a set of rotations about the joint axes that defines the geometric state of the joint at each sample [14]. IMUs track absolute orientation by integrating angular velocity, a quantity that they can directly measure by using a three-axis gyroscope. They may also find the absolute orientation through monitoring the local magnetic field surrounding the IMU, which provides an absolute reference for orientation if the magnetic field is uniform. The IMUs that will be used for our project have this capability. Producing joint angles from IMU data can be challenging, due to the nature of the sensors in an IMU and how the package interfaces physically with the human body. The greatest challenges in implementing an algorithm to produce joint angles from IMU data are drift, magnetic interference, and misalignment of coordinate axes.

Drift in IMU-reported absolute orientations and locations occurs because rate measurements from the IMU are integrated to produce the absolute orientations and locations. Any error in the measurement of instantaneous acceleration or angular velocity propagates through to and builds up within the integrated value. Errors in rate measurements can come from a variety of sources, including white noise and imperfect calibration (bias error). Errors in measurement of angular velocity mostly originate from these sources [15]. Acceleration measurement suffers from both sources of error, but most of the error comes from gravity compensation. To provide accurate acceleration measurements, the gravity acceleration vector must be subtracted from the measured acceleration value. Since the gravity vector in the IMU's local coordinate frame is dependent on the orientation of the sensor, error in orientation causes inaccuracy in gravity compensation. This is the greatest source of error in IMU-reported velocities and locations [15]. Over time, errors in rate measurements add up to produce an ever-increasing error in the integrated value. Angular velocity must be integrated once to produce absolute orientation, while acceleration must be integrated twice to produce an absolute location. Because of this, IMU-reported locations are especially susceptible to drift error from integration.

One way to mitigate the drift error in orientation is to use a magnetometer to measure the direction of the magnetic field of the Earth, which in theory provides a static reference for orientation in two axes. However, the accuracy of the reported absolute orientation from this method is contingent upon the magnetic field being uniform across the entire space in which the IMU is used. In reality, environments where IMUs are likely to be used contain many potential sources of interference. Electric cables produce a magnetic field due to moving electric charges [16], and if the cables are carrying alternating current as they do in the walls of buildings, the magnetic field produced also alternates. Another source of interference is ferromagnetic objects in the environment. Ferromagnetic metals magnetize in a magnetic field, affecting the magnetic field around them. If a ferromagnetic object moves within the environment, the magnetic field may be affected in a way that produces error in magnetometer readings. Therefore, no ferromagnetic objects should be moving, especially near the IMU, as data is being taken [16].

Another challenge that extracting joint angles from IMU data presents is that the IMUs are unlikely to be aligned exactly with the joint being measured. This is because, to avoid cumbersome preparation for experiments, IMUs are usually strapped onto the subject without much attention to their orientation. There are no convenient, well-aligned surfaces to attach the IMUs to, so fine positioning of IMUs is difficult. A representation of the complex geometry associated with this problem is shown in Figure 2 [14]. The algorithm must be able to "find" the joint location based purely on the data from the IMU. Most researchers use a process involving "calibration postures" to determine the joint direction in the IMUs' local coordinate system [14]. Subjects are asked to perform several predefined movements, and

the joint direction is calculated based on the IMU-reported absolute orientations of the body segments and the theoretical constraints defined by the posture. However, it is noted that the accuracy of these methods is limited by the ability of the subject to perform these movements precisely. Another method, proposed by Seel et al [14], is to use arbitrary motion data from the IMU sensors and exploit theoretical kinematic constraints, or physical limits of rotation, of the joints to calculate the joint axis directions. This method does not depend on the subject to perform specific movements precisely.

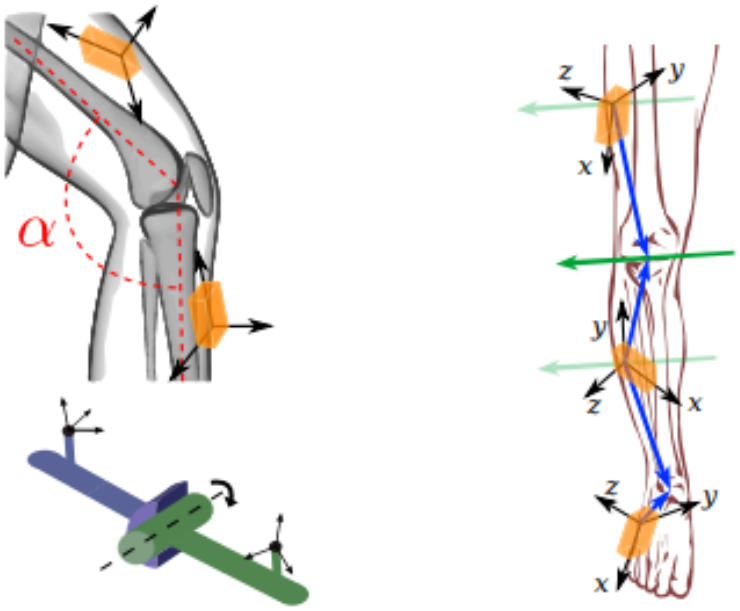

Fig. 2. IMUs applied to three body segments (upper leg, lower leg, and foot) can provide joint angle measurements despite being misaligned with the joint

Various IMU joint angle algorithms are produced using different methods of sensor fusion and making different assumptions about the measurement task. For example, a sensor fusion algorithm was used by Favre et al. [17] which used a combination of gyroscope and accelerometer readings to generate drift-resistant orientation measurements of the subject's body segments. The gyroscope readings were integrated to obtain an orientation, and the accelerometer reading was used as an absolute vertical reference to correct for the gyroscope drift. Subjects maintained a predefined standing posture to obtain the joint direction from the sensor data, which was used in subsequent experiments to obtain joint angles from the IMU data. Another algorithm used by O'Donovan et al. [18] made use of a magnetometer along with a gyroscope and accelerometer to produce joint angles. This method also made use of calibration postures to define the joint axis direction. Countless other methods have been used in the literature, and there are endless possible algorithms yet to be created. To evaluate the efficacy of joint angle estimation methods, a "ground truth" measurement of joint angles is required to compare against the angles reported by the algorithm. The goal of this project is to produce a portable device to provide the ground-truth data required to validate IMU algorithms.

Literature Search and Benchmarking

To better understand the problem and what exactly our team was tasked with, we held interviews with both Dr. Cain and our professor, Dr. Perkins, who are both experts on IMUs and their uses, as well as in adjacent fields and associated problems. Dr. Cain provided us with the groundwork on which the majority of our requirements and thus specifications were built, and Dr. Perkins helped clarify and further flesh out that groundwork. Dr. Cain also provided us with a paper [19] detailing a device that was created to have a very similar functionality to what he has requested of us, and that papers has informed many of our decisions.

After these interviews, we delved into the literature surrounding IMU validation devices and the associated areas to flesh out the project requirements and create their associated specifications. The following sources and benchmarks, while used to help define the requirements and specifications, were also informed by our preliminary ideas of the requirements. All of the finalized versions are shown in Table 4 in the next section on pages 9 and 10, and the related requirement for each source are called out as well.

In this research process we used several textbooks extensively. For our dynamics questions and calculations we referred to *Engineering Mechanics: Dynamics* [20], especially chapter 6 which was incredibly helpful in estimating the forces and torques to design for in Requirements 3 and 12 (pg. 9, 12).

When it came to the questions relating to the human body and joint movement, we referred to *DeGowin's Diagnostic Examination* [21] *and Biomechanics and Motor Control of Human Movement: Fourth Edition* [22]. These gave us information about joint kinematics allowing us to better visualize the end goal of the project, as well as providing insight into how design for human joint ranges and movement speeds, as shown in Specification 4 and 2, respectively (pg. 8, 10).

To further define what sorts of requirements would be expected of this device (perhaps ones that Dr. Cain and Perkins didn't mention) and to further develop a background of this area, we did some research into the performance of existing solutions on the market, which can be found below in Table 1. This information was used to generate Specification 1.

Table. 1. Systems used for benchmarking

System	Price (USD)	Error (˚)	Dimensions (H x L x W)	Portable?
State of the Art Videoradiography + X-ray W.M. Keck Foundation XROMM Facility at Brown University [23] [24]	800,000 +	0.09 [24]	~ 2.4 x 6.4 x 10 (m)	No
Standard Optical MOCAP	10,000 – 50,000	< 3 (depends on joint) [25]	N/A (governed by size of laboratory)	No
Optical Encoder ENC-A5SI [26]	60 ea.	0.072 (w/ quadrature)	~ 16.6 x 51.8 x 31.1 (mm)	Yes
Hall Effect Encoder	6.38 ea.	< 0.01	1 x 5.00 x 5.00	Yes

IC-MHQFN28 [27]			(mm)	
Angular Potentiometer NP24HS R10K L2% D5 [28] [29]	12 ea.	N/A (depends on ADC)	~ 7 x 24 x 24 (mm)	Yes

An additional benchmarking standard we used was the steps required for data acquisition in commonly used devices. Using this data, a practical number of steps could be applied and used for our device based off of similar products. Table 2 below shows the device type, the make and model, and the number of steps for five common devices. This information was used to generate Specification 11.

Table. 2. Data acquisition devices used for benchmarking

Device	Make/Model	Number Data Acquisition of Steps
Digital Camera [30]	Nikon D50	4
Cell Phone [31]	Moto G6	6
Arduino Board [32]	Arduino UNO	6
Raspberry Pi Board [33]	Raspberry Pi 4	5
Scanner [34]	HP Deskjet 2600 Series	4

To be able to decide how much our device should weight, we used some other daily portable devices as benchmarks as shown below in Table 3. This information was used to create part of Specification 6.

Table. 3. Devices used for benchmarking to determine the weight limit of our product

#	Device	Weight(kg)	Model	One-hand use?
1	Apple Remote Control [35]	0.05	Siri Remote	Y
2	Google Cell Phone [36]	0.1	Pixel 4a	Y
3	Swingline Stapler [37]	0.5	44401	Y
4	Make in Cookware Saucepan [38]	0.9	2QT	Y
5	Black & Decker Hand Drill [39]	1.2	BDCDD120C	Y
6	Dewalt Hand Drill [40]	1.5	DCD791D2	Y
7	Black & Decker Leaf Blower [41]	2.0	LB700	Y
8	WORX String Trimmer [42]	2.5	GT Revolution	N
9	Black & Decker Chainsaw [43]	3.4	LCS1020B	N
10	GoPro [44]	0.1	Hero 5	Y
11	iPhone [45]	0.2	11 Pro max	Y
12	MacBook Pro [46]	2.0	16 inch	Y

13	Dell Laptop [47]	2.5	XPS 17inch	Y
14	Camera shoulder mount [48]	7.0	Varizoom VZZGRIG	N

Using the various literature sources and benchmarking techniques covered in this section, we've been able to provide conventional backing for our requirements and specifications, which are detailed in the following section.

Requirements and Engineering Specifications

After defining the problem and gathering information to build a background knowledge to build off of, we worked closely with Dr. Cain to develop a list of requirements that we needed to design for. From that list of requirements, we created engineering specifications that necessarily achieved the requirements while also quantifying them in a measurable way. These requirements and engineering specifications are shown below in Table 4 and further details and justifications for each of them are given below it.

Table. 4. Project Requirements and Specifications

	#	Requirements	Engineering Specifications
Tier 1	1	Sufficient resolution of orientation between links	• Measure Euler angles of links to within ± 1°
	2	Sample fast enough for human motion	• Sample at a rate of ≥ 60 Hz
	3	Sufficient joint strength (static failure)	• Able to function under torques < 3 Nm
	4	Runs through ranges of motion of all human joints	• Can move 180 degrees along all three axes
	5	Sufficient data storage	• > 54 MB of storage
	6	Portable	• Maximum weight of 2 kg • Each end link length between 5" and 12" • Battery-powered for ≥1 hr on one charge
Tier 2	7	No interference with IMU magnetometer	• No materials that change magnetometer reading by > 0.1%
	8	Three (lockable) degrees of freedom	• Can move in 3 degrees of freedom with the capability of locking any of them
	9	Durable (fatigue failure)	• Can survive 1200 hours of use

	10	Repeatable IMU connection	• At least two orthogonal surfaces at attachment sites which locate IMUs within a tolerance of ± 1˚
Tier 3	11	Easy data acquisition	• Data acquired from device to computer in a maximum of 4-6 steps
	12	Firmly mount to a rigid structure	• Contains a mechanism able to connect the apparatus to a rigid structure under a force of 8 N in any direction

Tier One

These are the highest ranked specifications and are listed as such due to their fundamental importance to the project. Without these specifications the apparatus either wouldn't function well enough to be of any use in comparison to IMU data (this includes overall error, sampling rate, and mechanism strength) or wouldn't fulfill the desired use case of Dr. Cain's experimentation and thus wouldn't be useful to him (this includes the necessary range of motion, data storge, and portability).

Requirement 1: Sufficient resolution of orientation between links
Specification: Measure Euler angles of links to within ± 1°

As a starting point, Dr. Cain suggested that our device be capable of measuring angles with an accuracy of ± 1°. To justify this level of error, we normalized it by the minimum range of motion (ROM) we expect to measure [19]. The ROM used in our calculation is that of shoulder abduction/adduction during wheelchair propulsion which is equal to 16° [49]. This ROM was used because it is small compared to other movements, and Dr. Cain has an interest in studying this particular motion. When normalizing the sensor error by the minimum ROM, we get an acceptable percent error of 6.25% (Eq. 1).

$$\frac{error}{ROM} = \frac{\pm 1^\circ}{16^\circ} = \pm 6.25\% \quad (1)$$

Requirement 2: Sample fast enough for human motion
Specification: Sample at a rate of ≥ 60 Hz

A key specification for any measurement apparatus is the rate at which it is capable of sampling the signal it is attempting to measure. As a starting point, the minimum sampling rate should be equal to at least twice the frequency of the signal being examined. This principle is known as the Nyquist frequency [22]. In reality, you should aim to sample at a higher rate than the Nyquist frequency to improve signal fidelity. A literature search of human motion studies surveying a variety of movements including both lower and upper limbs, revealed that the most human movement occurs at frequencies below 6 Hz [22], [49], [50]. In order to adequately capture the maximum frequency of 6 Hz we chose a sampling rate of 60 Hz. This is five times above the Nyquist frequency of 12 Hz and is easily achieved by off-the-shelf microprocessors making it suitable for our application [51].

Requirement 3: Sufficient joint strength (static failure)
Specification: Able to function under torques < 3 Nm

This requirement is necessary to ensure the "joint" we create will be able to handle the torques that the accelerations of the links will create. We estimated the specification using the angular acceleration (α) achieved by the human upper arms and forearms during walking and running (2000 ˚/s^2) [52]. We then estimated the moment of inertia to be that of a thin beam rotating around its end (Eq. 2). Making certain estimations based off of our specifications (length (L) of 12 in and mass (m) of 2 kg), we calculated a preliminary moment of inertia (I), and then, using Equation 3, calculated the torque (τ) the joint would experience from that acceleration.

$$I = \frac{1}{3}mL^2 = 0.0619\ kgm^2 \quad (2)$$

$$\tau = I\alpha = 2.16\ Nm \quad (3)$$

We rounded the calculated torque up to 3 Nm to stay conservative. We don't imagine this specification will be difficult to achieve as 3 Nm is a fairly small torque value for our purposes, and our joint will likely possess very little friction.

Requirement 4: Runs through ranges of motion of all human joints
Specification: Can move 180 degrees along all three axes

This requirement is needed to be able to take measurements about all human joints. Since the maximum range of motion that a human joint can achieve is 180°, as shown in Figure 3 below, we came up with the specification that our device needs to be able to move 180 degrees along all three axes.

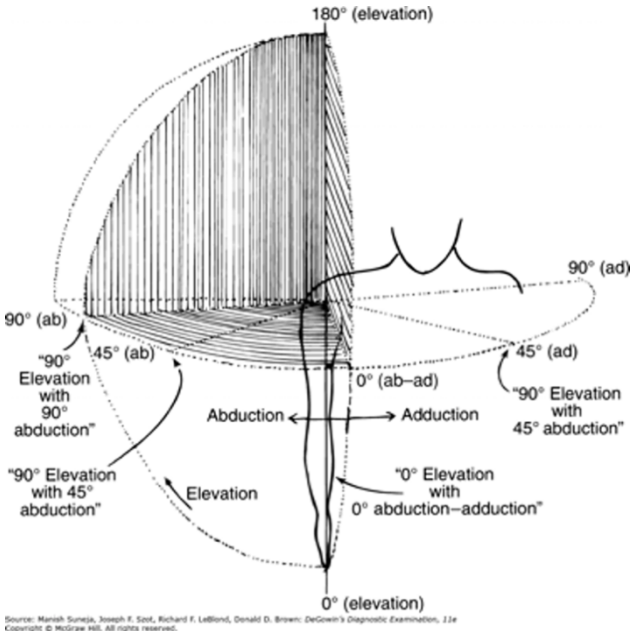

Fig. 3. Range of Motion of Shoulder Joint

Requirement 5: Sufficient data storage
Specification: > 54 MB of storage

An upper bound for the required minimum data storage capacity was found by generating a CSV file with the proper data columns: the sample timestamp and rotation in three axes. The device's charging period will serve as a convenient time to transfer files, so only the data taken during a full depletion of the battery will need to be stored. Because of this, the file contained the maximum expected number of collected data points as determined by multiplying the maximum battery life from Requirement 5 by the sample rate from Requirement 2. The CSV file format was used because it is text-based and memory-intensive, providing a high estimate for file size. The CSV format is also widely used, and so the data should be easily accessible to any user. The resulting file was 54 MB in size, so the device will require that amount of memory.

Requirement 6: Portable
Specifications: Maximum weight of 2 kg
Each end link length between 5'' and 12''
Battery-powered for ≥1 hr on one charge

Portability can be restricted by how much the device weighs. If the device is too heavy, it will be hard for the participant to work with for an extended period. Therefore, we came up with the number 2 kg as the weight limit based on the benchmarking of the weight of different portable devices on the market, as shown previously in Table 3.

Portability can also be restricted by its dimensions. The device needs to be small enough to be carried and managed by one person without assistance. The specific end link length range of five to twelve inches was chosen based on the average lengths of the human clavicle and humerus bones [53],[54]. Human shoulder joint mechanics are one of the areas of research that Dr. Cain's lab has worked on, so by keeping our apparatus to a similar size, our sensor technology and setup could potentially be implemented down the road with a wearable instrument.

Another aspect of portability that was identified was our instrument's need to function without being connected to a power source during use. Using battery-powered devices allows for this freedom. Dr. Cain specified that he'd like the instrument to take data for an extended range of time, with a minimum range of 1 hour. As mentioned above on page 4 in the background section, drift occurs because small errors in the IMU measurements are integrated. The longer data is recorded, the more this integrated error affects the IMU readings, so by taking data over a significantly large time range (of which ≥1 hour qualifies), Dr. Cain's lab will be able to see when IMU drift takes place throughout the recording which will help them determine the validity of their algorithms with respect to accounting for it [15].

Tier Two

These specifications are considered moderately important. The project could be completed without them and would yield useful data, but with certain flaws that should be avoided and would likely influence *how* useful the results end up being. This tier includes magnetometer interference, the lockable degrees of freedom, and the durability of the mechanism.

Requirement 7: No interference with IMU magnetometer
Specification: No materials that change magnetometer reading by > 0.1%

This requirement is necessary to avoid the presence of magnetic field distortion around the IMUs. Many IMUs are equipped with magnetometers (including the ones used by Dr. Cain), and without reliable magnetic field measurements, it's difficult to account for the drift of the IMU measurements (this is described in more detail on pages 5-6). Ferromagnetic metals can change the natural magnetic field [1], and if large amounts of those materials were used in our design, it would permanently distort the field around the IMU, always compromising the magnetometer measurements and thus the drift error corrections, leading to incorrect angle measurements. Thus, we chose 0.1% to ensure any change is negligible.

Requirement 8: Three (lockable) degrees of freedom
Specification: Can move in 3 degrees of freedom with the capability of locking any of them

3 degrees of freedom (DoF) are required to simulate any joint on the body given that the max DoFs of any anatomical joint is 3 (e.g. hip or shoulder joints). The ability to lock any given DoF on the measurement device is an added feature requested by Dr. Cain. This feature is useful for testing IMU algorithms that exploit kinematic constraints of different joints (see pg. 4) during the calibration process [55], [56].

Requirement 9: Durable (fatigue failure)
Specification: Can survive 1200 hours of use

This specification is necessary as a way to quantify durability by fatigue failure. As our instrument is not meant to be something that is in use all of the time, Dr. Cain requested that the device last for 20-60 experiments per year over the course of 5 years, which at most is 300 experiments, and he said this would be for experiments that lasted on average for 4 hours. Successful designing to meet this requirement will be achieved by choosing materials that are not prone to deformation and propagation due to fatigue.

Tier Three
These are our least important specifications. They consist mostly of additional features that would be beneficial, but the design would likely function well without them. These include the various connection features as well as the ease and simplicity of the data acquisition.

Requirement 10: Repeatable IMU connection
Specification: At least two orthogonal surfaces at attachment sites which locate IMUs within a tolerance of ± 1˚

Having a consistent placement of the IMU will help eliminate error coming from the physical setup. This way, if errors are detected in the IMU reading, coordinate axis misalignment can be ruled out [19]. This will help to better keep track of the IMU coordinate systems. The goal is to create a repeatable experiment situation within ± 1˚ because, by the specification for Requirement 1, we are constrained by ± 1˚ of error, and thus by staying below that error the overall increase in error will be very small.

Requirement 11: Easy data acquisition
Specification: Data transferred from device to computer in a maximum of 4-6 steps

The data acquisition of our instrument's data to a computer should not be overly complex. We want this process to be simple to benefit the end user. We determined that 4-6 steps is a common range of steps for devices such as cameras, phones, Arduino boards, Raspberry Pi boards, and scanners. These devices were surveyed as standard devices that underwent data transfer processes and are shown in the benchmarking section in Table 2.

Requirement 12: Firmly mount to a rigid structure
Specification: Contains a mechanism able to connect the apparatus to a rigid structure under a force of 8 N in any direction

Dr. Cain requested we design a method of mounting our apparatus to a rigid structure. This will make it easier to manipulate when it's being used statically. We used the same process as the joint strength torque calculations (Eq. 2, Eq. 3) as well as Equation 4 (shown below) to find the force being applied at the end of the end of the beam at maximum acceleration.

$$F = \frac{\tau}{L} = 7.087\ N \tag{4}$$

We rounded this value up to 8 N to be conservative. We don't imagine this will be very difficult to achieve as 8 N is a relatively small value in the context of our project.

Concept Generation

Categorization

The concept generation process began with a categorization of the design considerations expected to form complete solutions for the project. This project lends itself to a piecewise design process, as there are many different design considerations that have very little effect on one another. For example, the design of the joint has no direct effect on the material an end-link is made from, and the mechanism for locking degrees of freedom has no effect on the method used to offload data from the device. With this in mind, eight mostly independent overall categories for design considerations were developed. They are as follows:

1. Angular Sensor: This consideration involves choosing the optimal angular sensor for the device. The requirements involved with this design consideration are Requirements 1, 4, 6, and 7.
2. Joint Design: This consideration involves choosing the optimal joint design or configuration for the device. The requirements involved with this design consideration are Requirements 3, 4, 7, 8, and 9.
3. Degree of Freedom (DoF) Locking: This consideration involves choosing the best way to selectively prevent the movement of the joint in certain axes for certain use cases. The requirements involved with this design consideration are Requirements 6 and 8.
4. End-Link Features: Material. This consideration involves selecting the optimal material for constructing end-links. The requirements involved with this consideration are Requirements 6, 7, 9, and 12.

5. End-Link Features: Additional Features: This consideration involves selecting extra features to ensure the device is convenient to bring to locations outside of the lab. The requirement involved with this consideration is Requirement 6.
6. Data Acquisition: This consideration involves choosing a convenient method for storing and transferring collected data to a computer for further processing and analysis. The requirements involved with this consideration are Requirements 5 and 11.
7. Connection Mechanism: Rigid Body. This consideration involves choosing a robust method for attaching the device to a static body, such as a table or bench. The requirements involved with this consideration are Requirements 7, 9, and 12.
8. Connection Mechanism: IMU. This consideration involves choosing a secure, repeatable method for attaching IMUs to the end links of the device during experiments. The requirements involved with this consideration are Requirements 7 and 10.

Additionally, two of the eight categories were selected as most important. The first important consideration was *Consideration 1, Angular Sensor*. This consideration was prioritized because the angular sensor will define the precision of the device. If an improper angular sensor is chosen, the device will not function as required according to Requirement 1, a Tier 1 requirement. The second important consideration was *Consideration 2, Joint Design*. This consideration was prioritized because the joint design will define the durability and movement freedom of the device. If an improper joint design is chosen, the device will not function as required according to Requirements 1, 2, and 4, all Tier 1 requirements, and Requirements 7 and 9, both Tier 2 requirements. In addition, these design considerations seemed to be potentially the most difficult to produce solutions for that properly satisfy all the requirements. These categories were prioritized above the rest, so a larger proportion of the time spent in concept generation, development, and evaluation was spent on them compared to any other category. Selecting the correct option for these specific considerations was imperative to the success of the overall design, so spending extra time on them was likewise critical to the success of the project.

Brainstorming

With all design considerations categorized, the team held a brainstorming session to explore the design space. The goal of this meeting was to generate as many ideas as possible, regardless of any judgements we may have from previous experience or intuition. To generate ideas, we used divergent thinking, expanding on others' ideas, and synthesis as our main techniques. About 90 ideas were generated in total across all the design consideration categories. A complete list of generated design concepts can be found in Appendix B.1. As discussed previously, most of the concept generation time and effort was aimed toward the "top two" design considerations.

The brainstorming session began with a set of blank documentation materials, namely a word processing document with headings for all eight of the top-level design considerations and several sheets of unmarked sketching paper. We moved through each heading sequentially, spending an average of fifteen minutes on each one. During our visit to each heading, we began by listing all initial ideas for the related design consideration. To encourage creativity, some clearly infeasible but intriguing ideas were added to the mix. Novel ideas were periodically formed and posited by each group member, which the notetaker then added to the appropriate heading as the rest of the group continued to discuss them. An idea proposed by one group member often sparked the formation of ideas for other group members, leading to a significant amount of cross-pollenated ideas. The result was a comprehensive list of ideas for a given design consideration that spanned a variety of regions of the design space.

To improve communication of the ideas, some ideas were sketched. Two examples of angle measuring method sketches are shown below in Figure 4, and some additional sketches can be found in Appendix B.2.

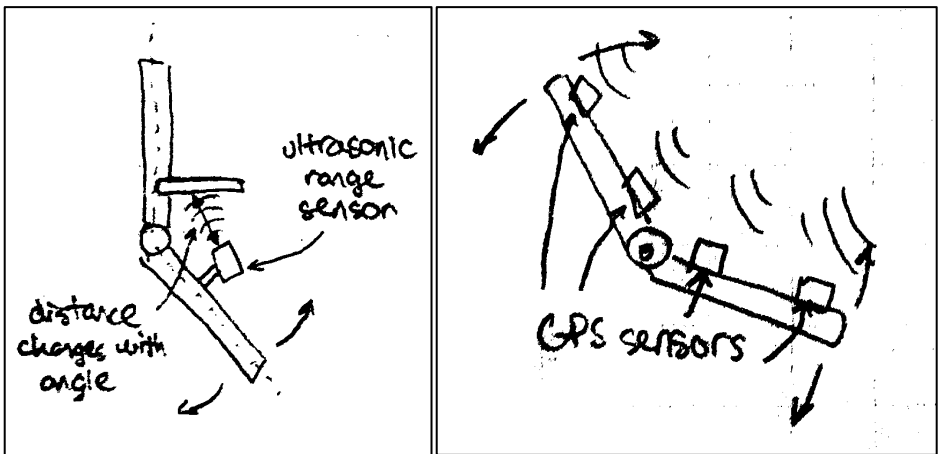

Fig. 4. Sketch of angle measurement using an ultrasonic range sensor (left), sketch of angle measurement using highly accurate GPS receivers (right)

Sketching the design concepts during the ideation session improved the group's comprehension of the less-intuitive ideas posited by individual members. For example, it was not initially clear how the GPS-related concept shown in Figure 4 would operate, given that GPS sensors are spatial location sensors and not orientation sensors. The sketch helped to show that an orientation could in theory be determined by compositing the locations of two GPS sensors on each link.

In all, the brainstorming session left the team with a large quantity of design concepts across all major design considerations. It also increased each member's understanding of design concepts in regions of the design space that they had not considered. However, these concepts were very preliminary and required further development to be evaluated on their ability to fulfill the design requirements. In addition, details of the concepts could be modified to produce more concepts with different advantages and disadvantages. To further explore the design space and develop the brainstormed ideas, the concept development stage began.

Concept Development

Design Heuristic Cards

To further develop new and different ideas, Design Heuristic cards were used. Design Heuristic cards are a compilation of 77 ideation prompts that promote out-of-the-box thinking when generating and developing concepts. [57] Figure 5 below shows the 77 prompts of design heuristic cards.

1. Add features from nature
2. Add gradations
3. Add motion
4. Add to existing product
5. Adjust function through movement
6. Adjust functions for specific users
7. Align components around center
8. Allow user to assemble
9. Allow user to customize
10. Allow user to reconfigure
11. Animate
12. Apply existing mechanism in new way
13. Attach independent functional components
14. Attach product to user
15. Bend
16. Build user community
17. Change contact surface
18. Change direction of access
19. Change flexibility
20. Change geometry
21. Compartmentalize
22. Convert 2-D to 3-D
23. Convert for second function
24. Cover or remove joints
25. Cover or wrap
26. Create system
27. Distinguish functions visually
28. Divide continuous surface
29. Elevate or lower
30. Expand or collapse
31. Expose interior
32. Extend surface
33. Extrude
34. Flatten
35. Fold
36. Hollow out
37. Impose hierarchy on functions
38. Incorporate environment
39. Incorporate user input
40. Layer
41. Make component multifunctional
42. Make components attachable or detachable
43. Make product resuable or recyclable
44. Merge functions with same energy source
45. Merge surfaces
46. Mirror or array
47. Nest
48. Offer optional components
49. Provide sensory feedback
50. Reconfigure
51. Recycle to manufacturer
52. Reduce material
53. Reorient
54. Repeat
55. Repurpose packaging
56. Reverse direction or change angle
57. Roll
58. Rotate
59. Scale up or down
60. Separate parts
61. Slide components
62. Stack
63. Substitute
64. Synthesize functions
65. Telescope
66. Texturize
67. Twist
68. Unify
69. Use alternative energy source
70. Use common base to hold components
71. Use continuous material
72. Use human-generated power
73. Use multiple components for one function
74. Use packaging as functional component
75. Use recycled or recyclable materials
76. Utilize inner space
77. Utilize opposite surface

Fig. 5. List of Design Heuristics' 77 ideation prompts

We generated the following seven different ideas based on the prompts from the Design Heuristic cards:

- (11) Allow User to Reorient: Have an external base with links that move independently. There would be no joint in between but rather a base with two links connected and the link positions would be measured relative to the base.
- (20) Change Geometry: Evaluate our angles using quaternions rather than Euler angles.
- (36) Fold: Make our end links foldable to increase portability.
- (40) Incorporate User Input: Have motorized end links that were controllable by the user.
- (42) Make Components Attachable/Detachable: Design the joint and links to be separate pieces that can be disconnected from each other to increase portability.
- (48) Nest / (65) Telescope: Use links that can collect their length into a small section of the link. Nesting would have pieces of the link that could separate and be stored inside of the link, where telescoping would have a single piece of the link that is collapsible.
- (58) Scale Up or Down: Create small scale measurement device so that there is less error that could come as a result of deformation is links or distance between IMUs and sensors.

Morphological Chart

We also used a morphological chart as a method of generating more ideas. With categories of problems listed out from brainstorming, we made a table, as shown in Appendix B.3, with each row representing one of the categories, and filled in many of possible solutions that we came up during the brainstorming section while also generating new ones. In the end, the combinations of solutions from each category formed the solution pool for the main problem as defined in the problem definition stage. Using Excel's random function, the index of each solution was used to generate unbiased solution combinations. For

example, one of the possible solution combinations we created was 336361133, which represents using angular potentiometer as the angle sensor, a ball and socket as the joint with no actuators, 3D printed links with foldability, SD card as the data acquisition method, pins for DoF locking, and clamp for both rigid body and IMU connections. Another solution combination we created was 171311244, which represents using optical encoders as the angle sensors, a hinge as the joint with electric actuators, 3D printed links with foldability, a cable as the data transfer method, pins for DoF locking, and screws for both rigid body and IMU connections.

While making the Morphological Chart, we also used a technique called cross-pollination, which is combining the ideas of different individuals with different ways of thinking to generate innovative solutions. For example, while suggesting certain solutions for rigid body connection, we realized many of those same solutions could also be used for the IMU connection, cross-pollinating between our design categories.

Gap and Bias Identification

Beyond developing and combining the ideas we already had to create more and superior solutions to our problem, we also decided to analyze the array of ideas we came up with, and point out specific gaps we missed, or biases that effected the fullness to which we explored certain areas. This led us to identify two main areas that weren't fully explored: complex designs and designs outside of mechanical engineering. Below is a more thorough definition of those two areas and an explanation of some of the ideas we came up with after more thoroughly exploring these spaces.

First, complex designs. Reflecting on our design generation process, we became aware that we were frequently avoiding or not thoroughly considering designs that added a lot of complexity. This was partially due to our desire to choose something that would be easier to design and potentially build given the constraints of the semester (this one especially with the in-person aspects ending several weeks earlier). To counteract this, and ensure we didn't eliminate perfectly viable options, we spent a while simply attempting to brainstorm ideas inside of this gap. This lead us to potential additional features that could be added, such as fusing the sensor data from our angle sensors and the IMUs that will be attached in the future to allow for easier data analysis. We also more seriously considered how we could motorize the mechanism allowing for more exact movements that mimic human motion and even considered increasing the accuracy of our sensors by implementing a feed forward loop of sorts using neurological signals.

Second, designs outside of mechanical engineering. Looking through our designs we realized from the start that we had begun with the idea of a physical mechanism with mechanical properties and solutions almost immediately. This was largely due to how Dr. Cain posed the problem, as well as our academic backgrounds and expertise, but we still felt it pertinent to explore a little bit of the space outside of purely our discipline. This led us to a brainstorming session with no "comfortable" mechanical designs allowed. Doing this led to us finding a capacitive sensor to measure joint angles, the idea of doing further biological modeling and prototyping of a shoulder and using that as the base structure for our mechanisms to more accurately model human motion, and even considering how we could measure the dynamics of fluid surrounding the mechanism during motion to back out joint angles that way.

While we didn't end up selecting any of these for our final design, for many of the same reasons we initially missed the design space originally, we felt like we better understood the problem, and the scope of potential solutions after further exploring these sections. This led us to make more informed and complete decisions in the next phase: evaluation and selection.

Concept Evaluation and Selection

In the concept evaluation stage, we applied a four-step process to narrow down our extensive lists of ideas created during concept generation. First, we attributed engineering requirements to each of the eight design categories defined on pages 14-15. Second, we simply applied common sense to quickly eliminate ideas from each category that clearly did not meet all applicable engineering requirements. For example, using X-Rays and video radiography to measure joint angles may provide high measurement accuracy but using large X-Ray machines is impractical given our portability requirement so we could quickly dismiss it without detailed benchmarking. Third, once we had narrowed down each design category to 3-5 top ideas that had potential to meet all their respective requirements, we used Pugh charts to help choose a final concept for each category. Finally, we did a gut check regarding both the individual performance and the synergy of all the final design choices.

The criteria used to rank ideas in Pugh charts are a combination of both engineering requirements as well as secondary considerations to help differentiate similar ideas. For example, *measurement error*, *portability*, and *magnetic material* are all criteria for the angular sensor Pugh chart that directly correspond to engineering requirements 1, 6, and 7. However, additional criteria like whether the angular sensor is “contactless” is also included to act as a lower weighted criteria to differentiate similarly preforming sensors (we made sure to stay cognizant of sensitivities to the weights in our chart during this process). It should also be noted that our Pugh charts do not include a baseline column of all zeros. While this is a common way to construct a Pugh chart, we did not want to arbitrarily force one design to have zeros for all criteria. Consider the situation in which the baseline design performs exceptionally well for a certain criterion and is forced to take a zero. Now, all other competing designs must receive a -1 for that criterion which is a misleading representation of each design’s performance. To avoid this, we opted for a scoring system where a +1, 0, or -1 was assigned to every criterion for every design being compared based of an internal baseline we had developed from our research and benchmarking. Also, it should be noted that nearly every requirement has some effect on every one of these categories. To ease the analysis without compromising the result, we focused on the requirements that had the largest effect on a given category.

To combat any biases that inevitably occurred during the Pugh chart analysis, we performed further evaluation to ensure robust design selection. For our next screening stage, we did a gut check of the Pugh chart results based on our engineering experience and our stakeholder’s opinions. If no red flags were raised about the individual design choices, we then examined our device at a systems level. This primarily consisted of another gut check based upon intuition, however one important tool we leveraged during this process was CAD. Having the ability to visualize all three of our high-level joint designs allowed us to easily spot flaws in the overall system. For example, our ball and socket joint has an advantage of not exhibiting any singularities, however, it would be very difficult to integrate angular sensors capable of measuring its different DoFs which becomes very apparent during a CAD review.

As previously mentioned in the concept generation section on page 14-15, two of our eight design categories, angular sensors and joint designs, were given special priority due to their large impact on Tier 1 engineering requirements. These two foundational categories were appropriately evaluated with a higher level of detail relative to other categories and include things like benchmarking tables and CAD renderings.

Foundational Categories

Angular Sensor

The angular sensor is arguably the most important design choice given our project's chief goal is providing ground truth orientation data. After compiling a list of over thirty different methods for measuring angles, we narrowed down our focus to three types of sensors: optical encoder, angular potentiometer, and hall effect encoder. These sensors were chosen because they all had potential to meet our engineering requirements for *angle resolution*, *range of motion*, *portability*, and *magnetic interference* (Requirements 1, 4, 6, and 7).

Given that angular sensor type is a foundational design category, detailed benchmarking was performed which included at least one sensor for each of the three types. Sensor specifications that relate directly to engineering requirements are shown below in Table 5, while specifications pertaining to secondary features are shown in Table 6. Note that *power supply* was included in Table 5 with the rationale that low power devices are more portable, thus corresponding to Requirement 6.

Table. 5. Angular sensor specifications directly related to engineering requirements

Angular Sensor Type	Total Error (deg)	Resolution (deg)	Dimensions (mm) (H x L x W)	Power Supply (V)	ROM (deg)	Magnetic
Optical Encoder [58]	~ 0.29	0.29	~ 17 x 52 x 31	5	360	No
Potentiometer [59]	~ 3.44[a]	0.04[b]	~ 30 x 20 x 20	N/A	340	No
Hall Effect [60]	0.05[c]	0.02	~ 10 x 28 x 22	5	360	Yes
Hall Effect [61]	0.25	0.02	~ 45 x 45 x 30	5	360	Yes
Capacitive Encoder [62]	0.20	0.02	~ 15 x 42 x 48	5	360	No

[a] Potentiometer error dominated by non-linearity, [b] Resolution calculated for 13-bit ADC, but could be driven even lower if higher bit ADC was used [c] Minimum error assuming linearization and averaging are performed by external microcontroller

Table. 6. Secondary features and specifications for angular sensors

Angular Sensor Type	Embedded ADC	Absolute[a]	Contactless	Housing Included	Output Type	Cost $ (ea.)
Optical Encoder [58]	N/A	No	No	Yes	Digital	60
Potentiometer [59]	N/A	Yes	No	Yes	Analog	23
Hall Effect [60]	14 bit	Yes	Yes	No	Digital	17
Hall Effect [61]	14 bit	Yes	Yes	No	Digital	65
Capacitive Encoder [62]	N/A	No	Yes	Yes	Digital	33

[a] "Absolute" is used to refer to a sensors ability to know its angle relative to an inherent reference point without needing to perform a homing routine when powered on.

After the initial benchmarking of these four sensors, we constructed a Pugh chart shown below in Table 7 which includes criteria based on both Tables 5 and 6. Criteria derived from Table 5 is weighted higher due to the direct correlation to our engineering requirements. It should also be noted that the Pugh chart is not a direct one to one comparison of the preceding tables. For example, dimensions and power supply specifications found in Table 5, both correspond to the portability requirement and are therefore lumped into the portability criteria in the Pugh chart. *Total Error* is weighted highest at 5 due to its direct relation to the primary goal of our device – measuring orientation between two end links. *Portability*, *ROM*, and *Magnetic Interference* are all weighted at 4 given their direct correlation to other engineering requirements. Price was rated as a 3, since Dr. Cain had a fairly limited budget and wanted us to abide by it. The remaining criteria were weighted at 1 given that they are all beneficial features, but they are not necessary engineering requirements.

Table. 7. Angular Sensor Pugh Chart

Criteria	**Weight**	**Optical Encoder [58]**	**Angular Pot [59]**	**Hall Effect Encoder [60]**	**Hall Effect Encoder [61]**	**Capacitive Encoder** [62]
Total Error	5	0	-1	+1	0	+1
Portability	4	0	0	+1	-1	0
ROM	4	+1	0	+1	+1	+1
Magnetic Interference	4	+1	+1	-1	-1	+1
Cost	3	0	+1	+1	0	+1
Embedded ADC	1	0	0	+1	+1	0
Absolute	1	0	+1	+1	+1	0
Contactless	1	0	0	+1	+1	0
Housing Included	1	+1	+1	0	0	+1
Total		**+9**	**+4**	**+15**	**-1**	**+17**

From Table 7, it is clear the CUI Devices capacitive encoder [62] best meets our requirements. These decisions and the weightings were the compilation of several iterations as we re-evaluated what was most important.

Joint Design

During the diverging phase of concept generation, we had almost 30 ideas for this section. After using common sense, we quickly eliminated ideas such as literal magic and a literal human arm, only the pivot-hinge-pivot, universal joint with rotator, and ball-and-socket joint survived the screening-by-requirement stage. CAD models of each type of joint are shown below in Figure 6. The clamp structure (shown in green in the CAD renderings) is the potential locking mechanism for degree of freedom locking.

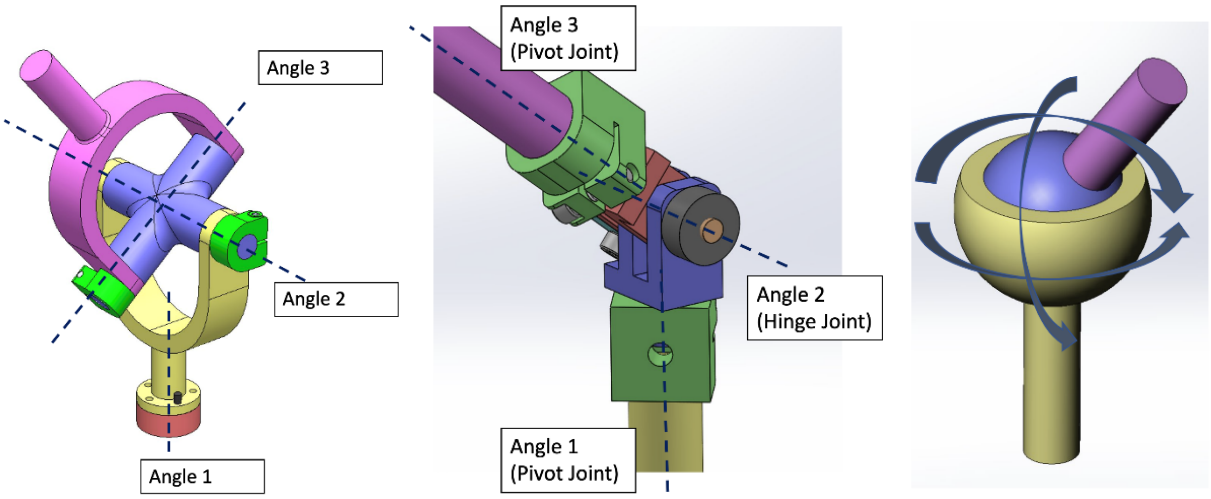

Fig. 6. Universal joint with rotator (left), pivot-hinge-pivot (middle), ball-and-socket design (right)

Each joint design has its own unique characteristics. The singularity is one of the more important criteria used to evaluate which joint is the most suitable for our device since it is directly related to requirement 4, which is to be able to cover ranges of motion for all human joints. Singularities are cases when the joint loses the ability to describe one of more degrees of freedom. This phenomenon occurs when two or more rotation axes line up with each other. Figure 7 shows the singularity of the universal joint and the pivot-hinge-pivot joint. In such case, angle 3 and angle 1 are aligned with each other, which makes it impossible to uniquely describe both angles. Due to this loss of information, joints with no singularities within the desired range of operation are preferred.

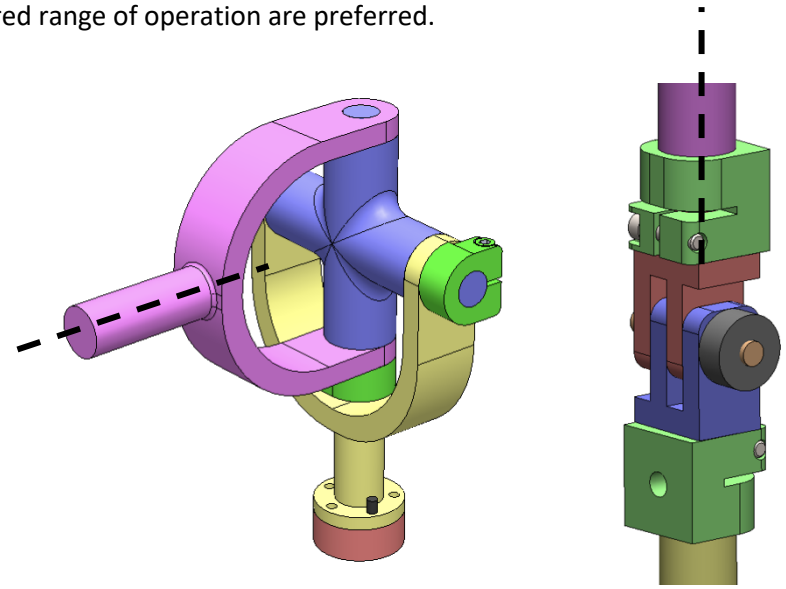

Fig. 7. Orientation of singularity for the universal joint (left) and for the pivot-hinge-pivot joint (right)

As shown above in Figure 7, the universal joint reaches its singularity at the boundary of the 180° range of motion, whereas the pivot-hinge-pivot joint reaches its singularity at the middle of its range of motion (90°). Therefore, the universal joint has a more favorable singularity compared to the pivot-hinge-pivot joint. Since the ball and socket joint has no singularity anywhere inside its range of motion, it out-performs both the universal joint and the pivot-hinge-pivot for this criterion.

Range of motion is another important criterion since as described in Requirement 4, the joint needs to have 180 degree of motion so that it can be used to study any human joint movement. The range of motion of the universal joint and the pivot-hinge-pivot joint is much larger than that of ball and socket joint. Even though the range of motion can vary by specific design, the ball and socket joint can never reach 180° without the ball falling out of the socket. The ball and socket joint shown in Figure 8 only has 70° of range of motion. The universal joint, on the other hand, can easily reach 250° and the pivot-hinge-pivot, 230°, as shown in Figure 8.

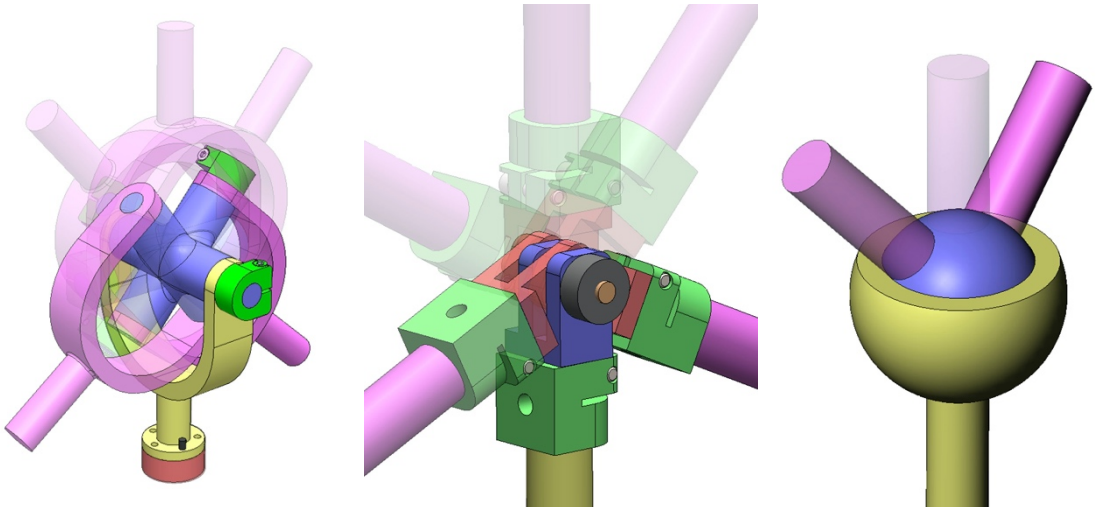

Fig. 8. The universal joint (left) and pivot-hinge-pivot joint (middle) have a larger range of motion than the ball and socket joint (right).

Including singularity and range of motion, all other criteria are listed in a Pugh chart with different weight assigned to them based on different requirement, as shown in Table 8. *Range (180°)* was given a 4 as without have 180° range of motion, it cannot cover the whole range of motion for human joint and therefore not suitable for collecting human movement data as described in Requirement 4. We gave *portability* a 3 since it is important for the participant to be able to use this device for ≥1 hour as described in requirement 6. We gave singularity a 3 as having a less significant singularity within the range of motion is helpful for realizing Requirement 4 fully. *Manufacturability* was given a 2 since if we actually want to build a prototype, under COVID-19, the options are really limited, however, since building a prototype is not required and manufacturability is also not required by our stakeholder, it was only given a score of 2. *Sensor Integration* was given a 3 as it indirectly affects the accuracy of angle measurement. This requirement is important because if it's hard to measure angle changes and we cannot directly attach the angle sensor to an axis of interest, any intermediate structure would induce extra error. Criteria *Lockability* was given a 3 as it was required by our stakeholder to have lockable degree of freedom. *Biological similarity* was given a 2 as it aids in the visualization and calculations of the joint angles but isn't necessary or required by our stakeholders.

Table. 8. Joint Design Pugh Chart

Criteria	Weight	Universal Joint with Rotator	Pivot-Hinge-Pivot	Ball and Socket
Range (180°)	4	+1	+1	0
Portability	3	+1	+1	+1
Singularity	3	0	-1	+1
Manufacturability	2	0	0	-1
Sensor Integration	3	+1	+1	0
Lockability	3	+1	+1	-1
Biological Similarity	2	0	-1	+1
Total		**+13**	**+8**	**+3**

As shown above in the Pugh chart, the universal joint with the rotator scored the highest. This result is not surprising given that the universal joint design has been successfully used in the past by another research team for a similar project.

Other Categories

Degree of Freedom Locking

This consideration involves choosing the best way to selectively prevent the movement of the joint in certain axes for certain use cases. The primary requirement associated with this design consideration is Requirement 8, which prescribes the ability to lock any of the three degrees of freedom to better emulate specific joints. Requirement 6 was also a minor consideration in this mechanism. Based on these requirements, the initial design concepts were narrowed down to the four shown in Table 9. For example, the "cord-tangling" concept was culled due to its lack of reliability and its potential operational difficulty for the user. The remaining concepts were then differentiated based on the criteria of tight locking, simplicity, and size. *Tight locking* was the highest priority and received a weight of 4 because any movement in locked axes could have a large effect on the IMU algorithm being tested if that algorithm is relying on certain kinematic constraints to produce its joint angle estimates. Additionally, this criterion aligns with Requirement 8, a Tier Two requirement. *Simplicity* received a weight of 2 because simpler mechanisms are easier to manufacture and often less prone to failure, but advantages in functional criteria should not be overpowered by lower simplicity. *Size* also received a weight of 2 because a smaller locking mechanism will help to maintain the portability requirement for the device, Requirement 6, but it is unlikely that any of the locking mechanism concepts to be evaluated will be large enough to significantly degrade the portability of the device. A Pugh chart was created to evaluate the design concepts based on these criteria and weights:

Table. 9. Degree of Freedom Locking Pugh Chart

Criteria	Weight	Pins	Screws	Modular Construction	Clamp
Tight Locking	4	0	0	+1	+1
Simplicity	2	+1	+1	-1	+1
Size	2	+1	+1	+1	+1
Total		**+4**	**+4**	**+4**	**+8**

Based on the scores from Table 9, the clear choice is to use clamps as the DoF-locking mechanism. While other concepts fail in one or more of the criteria, clamps perform in all three categories. They allow for tight locking, are simple and compact. This aligns with the initial evaluation of the concepts, in which the clamp was the favorite design concept.

End-Link Features

Next, we focused on the features of our end-links. These were split into two main categories: the material and additional features.

For the material, we narrowed down our focus, eliminating options such as paper and wood due to the greatly increased manufacturing processes and potentially durability, with very little other added benefit. Continuing on like this for all the other examples, we narrowed out selection to three commonly used materials: 3D printed PLA, aluminum, and acrylic, using our requirements and specifications (mainly 6, 7, 9, and 12). We then ranked these using criteria created from the same list of requirements and specifications, assigning weights based on their relative importance. *Weight* was given a weighting of 4, which is tied for the highest importance, because of its contribution to portability. *Manufacturability* was also given a weighting of 4 based on its importance to the ability to finish the product within the time and COVID constraints for this semester. *Structural integrity* was given a 3 as well since it's quite important for the function of the device, but not uneasy to achieve. *Sustainability* was given a 3 as we'd like to give a relatively high weight to our environmental effect during this project. And finally, *cost* was given a 2, as it's a factor, but not one of particular difficulty to achieve or importance to us. This set of materials, along with criteria and weightings are shown in Table 10 below along with sources for each relevant rating.

Table. 10. End-Link Material Pugh Chart

Criteria	Weight	3D Printed PLA	Aluminum	Acrylic
Manufacturability	4	+1	0	0
Weight [63]	4	+1	-1	0
Structural Integrity [63]	3	0	+1	0
Sustainability [64] [65] [66]	3	0	+1	-1
Cost [67]	2	0	0	0
Total		**+8**	**+2**	**-3**

The table shows that 3D printed PLA meets the most of our weighted criteria, so we have decided to use this material. From an efficiency perspective, 3D printing the linkages could likely be the difference between whether or not a prototype can be constructed with our time constraints and allows for increased iteration in building. For these reasons, we favored PLA strongly compared to the alternatives.

For the additional features subsection, we came to a list of four features: telescoping, nesting, folding, and detachable links. We arrived at these features using the methods described earlier, eliminating options such as attaching the mechanism to a drone, or making it rollable due to obvious logistical and manufacturing issues, as well as the incredible and unnecessary increase in complexity. Having narrowed down out list we come up with and ranked criteria based on our requirements, especially portability (Req. 6), determining similar criteria and weights for *manufacturability* and *weight* to before, while also adding *size* (ranked as a 2 based on the limited ability to improve portability only when not in use and in a relatively less useful way) and *joint specific adjustability*, or the ability to adjust the apparatus to better model a specific joint (ranked as a 3 based on the potential for improving IMU algorithms with certain simplifications added). This set of features, along with the criteria and weightings are shown below in Table 11. It's important to note that unlike in previous Pugh charts, these features are not mutually exclusive, and thus we used a cut off of zero for determining whether or not to include them.

Table. 11. End-Link Features Pugh Chart

Criteria	Weight	Telescoping	Nesting	Folding	Detachable
Manufacturability	3	-1	-1	-1	0
Weight	4	-1	-1	-1	0
Size	2	+1	+1	+1	0
Joint Specific Adjustability	3	+1	0	0	+1
Total		**-2**	**-5**	**-5**	**+3**

As can be seen in the table, the detachable feature is the only one that meets our net positive cutoff of zero or greater. During the creation of the CAD, we ran into some issues with the implementation of the detachable link, and thus decided not to include that feature either. These choices align with how we viewed our requirements as well, as implementing the size-reduction features (telescoping, nesting, and folding) will likely increase the weight, negating a lot of the benefit. Additionally, these features largely only increase portability while not in use which is a must less useful form of portability than when in use.

Data Acquisition

This consideration involves choosing a convenient method for transferring joint orientation data from our microcontroller unit (MCU) to a personal computer (PC). This design consideration directly corresponds to Requirement 5, which prescribes the data storage capacity, and Requirement 11 which prescribes the ability to easily acquire data. Various concepts on our original list of data acquisition methods were obviously over-complicated or impractical (e.g. quantum communication, morse code, Neuralink) and were quickly ruled out with a gut check based on Requirement 11. Printing data to a serial monitor and then copying to a static data file was also ruled out for complexity and its requirement of being tethered to a PC during collection which violates Requirement 6: portability. The remaining concepts on our initial list can be organized in two categories: wireless data acquisition, and

removable drives. The two most viable wireless options include using secure shell protocol to copy data files from our MCU to a PC or pushing data from our MCU to a remote file repository like Git. Two removable drives that offer potential solutions are USB flash drives and SD cards. Based on our engineering requirements we generated a Pugh Chart (shown below in Table 12) with three criteria to quantify the relative success of each data acquisition method: *Data storage capacity* weighted highest at 3 due to it corresponding to a Tier 1 requirement, *Ease of use* weighted at 2 since it corresponds to a lower tier requirement, and *Physical Size* weighted at 1 which relates to our portability requirement. Although portability is a tier 1 requirement, *Physical Size* was weighted lowest due to the minimal difference in size of all four options. It should be noted that similar to the End-Link Features Pugh chart, the different solutions for data acquisition are not mutually exclusive, therefore, any option with a positive net score is considered viable.

Table. 12. Data Acquisition Pugh Chart

Criteria	Weight	SSH	Git Repo	SD Card	USB Drive
Data Storage Capacity	3	+1	+1	+1	+1
Ease of Use	2	0	-1	+1	0
Physical Size	1	+1	+1	0	0
Total		**+4**	**+2**	**+5**	**+3**

We ultimately chose to utilize the SD card for data transfer, due to the built in SD card slot available to use on our microcontroller. This method is robust to poor internet connection or bugs in WiFi protocols common to microcontrollers, and it does not require the purchase of an extra component to act as a USB host (since our microcontroller is a USB slave).

Connection Mechanisms

Finally, we'll discuss our concept evaluation and selection for the connection mechanism categories. The first of these mechanisms involves connecting our mechanism to a rigid body (such as a table or other larger stable item). As explained in Requirement and Specification 12 (pg. 13), we need our mechanism to attach to a rigid body with a strength of at least 8 N. We narrowed our focus from the wide range of selections, eliminating options such as welding and arbor pressing due to increased complexity and lack of easy disconnection, to the subset of four ideas using the methods explained earlier. After finding our final subset, similar to the other categories, we created various criteria, along with their associated weights, based off of our requirements and specifications and their relative importance. *Interfaceability* (the ability for the connection to work on various types of surfaces surfaces) and *detach/reattachability* (the ability to remove and re-add the product) were given relatively high weights of 4 due to their integral importance to the actual function of the connection. *Strength* and *simplicity* (ease of manufacturing and design) were given relatively low importance (weights of 2) due to the fact that the necessary strength is quite low and thus will likely not be a factor and the simplicity is more focused on convenience than actually necessity. This subset, along with criteria and weightings is shown in Table 13 below.

Table. 13. Rigid Body Connection Mechanism Pugh Chart

Criteria	Weight	Clamp	Screws	Velcro	Pin
Interfaceability	4	+1	0	+1	0
Detach/Reattachability	4	+1	+1	0	+1
Strength	2	+1	+1	0	+1
Simplicity	2	+1	0	+1	0
Total		**+12**	**+6**	**+6**	**+6**

This table clearly shows that the clamp is the best option as it outranks all the others, while actually achieving a +1 in every criterion. This was no surprise to us as it seemed to fit all the requirements well from the beginning. The type and implementation of the clamp could look very different depending on how our end links end up looking, so more iteration with this design is in our future.

The next connection mechanism is the connection between the IMU and the end-links. As explained in Requirement and Specification 10 (pg. 13), we need a repeatable connection between an IMU one of our links to reduce error in their measurements due to misalignment. Similar to the previous section we narrowed our focus down to some of our more realistic ideas, eliminating similar options as before, and then developed criteria for them, along with weighting to judge their relative importance.

The ideas for this design are grouped into two subcategories: machined slot and machined corner. The first of these described a precision machined slot for a specific IMU with the subcategory of locking the IMU in place using a key of sorts that's designed to slide or screw in creating a fourth wall and locking the movement of the IMU. The second describes a precision machined corner in which an IMU can be consistently placed, while being connected through one of several methods (double sided tape, clamp or Velcro).

The criteria integral to our design and ability to adjust for different IMUs (*precision* and *interfaceability*) were assigned weights of 4 to emphasize that, as was *bulkiness* due to its importance to the portability requirement. *Ease of access* and *detach/reattachability* are of mid importance (weight of 3) as they provide a large amount of on-going convenience to connecting and disconnecting the IMU. At weights of 2, *strength* and *simplicity* are listed due to the ease in which strength can be achieved, and mostly one-time benefit of simplicity. All of this is shown in Table 14 below.

Table. 14. IMU Connection Mechanism Pugh Chart

Criteria	Weight	Machined Slot	Machined Corner		
		Key	Double Sided Tape	Clamp	Velcro
Detach/Reattachability	3	+1	0	+1	+1
Interfaceability	4	-1	+1	+1	+1
Precision	4	+1	0	0	-1
Ease of Access	3	-1	+1	0	+1

Bulkiness	4	+1	0	-1	0
Strength	2	+1	0	+1	0
Simplicity	2	0	+1	+1	+1
Total		**+6**	**+9**	**+7**	**+8**

This table shows that double sided tape is the best option. Based on the rankings it's clear it meets more of our weighting requirements than the other designs. Intuitively, this seems to be optimal to us as well, and was suggested by our stakeholder as a good option.

Engineering Analysis

After going through our various options for the different parts of our designs and selecting the ones best suited to our project, we began working on checking to make sure they met our specifications. In this section we've shown those methods and calculations for our three most important design drivers: Total error, range of motion, and portability. These were derived from some of our more important specs that weren't super simple to check.

Design Driver 1: Total Error

Our highest priority design driver was the total error of our angle sensor. This was chosen in accordance with our most important requirement (Req. 1): Sufficient resolution of orientation between links, which is defined as the Euler angles being within 1 degree. In order to preliminarily test this, we found all the different types of errors associated with our chosen sensor, the capacitive sensor shown in Tables 5 and 6, and added them in a root-sum-square (RSS) method [68].

The datasheet for this sensor lists two relevant values for this calculation. First, a maximum pre-quadrature pulses per revolution (PPR) of 4096, and second an overall accuracy error of 0.2 degrees.

We used Equation 5 below to calculate the resolution error of the sensor.

$$Error_{Res} = \frac{ROM}{PPR \times 4} = 0.0220^{\circ} \tag{5}$$

Then we used Equation 6 below to find the total error.

$$Error_{Tot} = \sqrt{{Error_{Res}}^2 + {Error_{Acc}}^2} = 0.2012^{\circ} \leq 1^{\circ} \tag{6}$$

This shows that the capacitive sensor we've chosen has the accuracy and resolution to achieve our specification of measuring the Euler angles of the links to within 1 degree.

Design Driver 2: Range of Motion

Our second design driver was the range of motion for our joint mechanism. This directly relates to our Requirement 4 which states that apparatus has to be able to rotate 180 degrees around all three axes. In order to test this, we used both low-fidelity prototyping and CAD modeling. Fig. 9 shows the general ideas used for these validation methods.

For the low-fidelity prototyping, we constructed a universal joint using cardboard to gain a better understanding of the way it functions. The prototype was able to rotate 180 degrees about each of its three axes, which increased our confidence in the use of a universal joint for our project requirements. Details of the construction of the low-fidelity prototype are outlined later in the report.

For the CAD modeling, we completed a full CAD model of our apparatus. To test the range of motion for each joint, the needed constraints and connections were added in SolidWorks. We then rotated the pieces in SolidWorks around each of the three axes to determine if there were any physical interferences between individual parts within the model. There were no part interferences, so the CAD model for our apparatus helped solidify that our universal joint design can achieve 180 degrees of rotation around each axis.

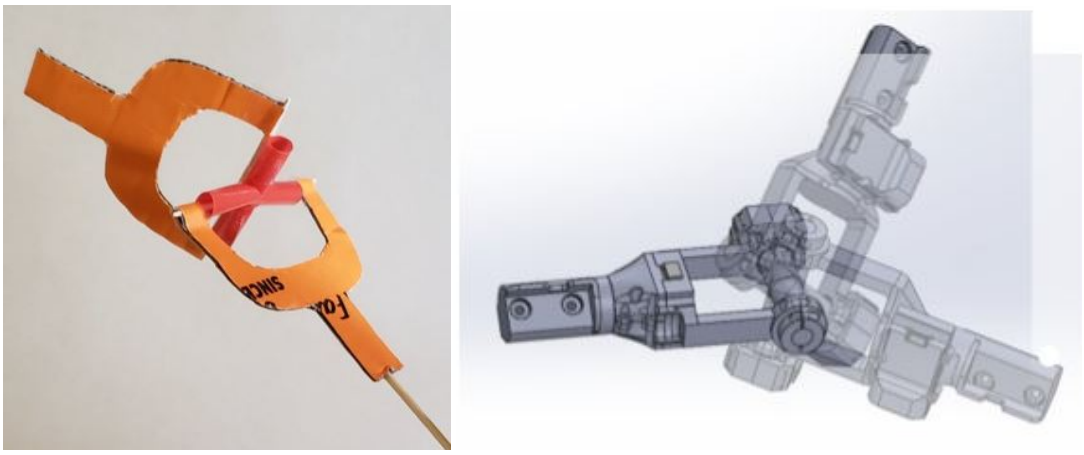

Fig. 9. The low-fidelity universal joint prototype (left) and the CAD model (right) used for testing range of motion.

Design Driver 3: Battery Life

Our third design driver was the portability of our device, which directly corresponds to Requirement 6. The primary analysis for this requirement concerned the battery capacity needed to power our device for more than 1 hour. Prior to performing this analysis, we tentatively chose a 4.4Wh Adafruit LiPo battery [69] we thought could potentially supply the necessary power. This initial selection was also based on the battery's ability to be recharged as well as its small form factor (dimensions of 34mm x 62mm x 5mm and a weight of only 23g) and low cost ($10).

Next we calculated the total power draw, P_{tot}, of our data acquisition system. This term is the sum of three different components: (1) P_{MCU}, the typical power consumption of the MCU (microcontroller unit) with no peripherals attached, (2) P_{CUI}, the power consumption of the three CUI capacitive encoders, and (3) P_{res}, the additional power dissipated by resistors in our battery charging module.

P_{MCU} is calculated using Equation 7 where $I_{dd\,1}$ is equal to 36mA. The value of $I_{dd\,1}$ is approximated from the Teensy 3.5 electrical spec sheet [70] which assumes that $V_{dd\,1}$ is 3.6V and the core frequency is 120MHz.

$$P_{MCU} = V_{dd\,1} I_{dd\,1} = 130mW \tag{7}$$

P_{CUI} is calculated using Equation 8 where $V_{dd\,2}$ and $I_{dd\,2}$ are provided by the CUI spec sheet [62] and are 5.5V and 16mA respectively. A factor of three is included to account for there being three sensors connected in parallel to V_{dd}. Additionally, an efficiency term, η, equal to 0.88 is included for the voltage booster that is required due to the differing logic levels of the MCU and angle sensors.

$$P_{CUI} = 3\frac{V_{dd\,2}I_{dd\,2}}{\eta} = 300mW \tag{8}$$

P_{res} is calculated using Equation 9 where V_{reg} is the MCU's regulated voltage equal to 3.3V, and R is resistance equal 330 Ohms. The whole quantity is multiplied by a factor of two since there are two resistors connected in parallel to V_{reg}.

$$P_{Res} = 2\frac{{V_{reg}}^2}{R} = 66mW \tag{9}$$

P_{tot} can now be calculated in Equation 10 by summing Equations 7-9.

$$P_{tot} = P_{MCU} + P_{CUI} + P_{Res} \approx 500mW \tag{10}$$

Finally, we calculate the battery life using Equation 11 where $\bar{P}_{bat}$ is the battery capacity equal to 4.4Wh.

$$\bar{P}_{bat} \div P_{tot} = 8.8\,h \tag{11}$$

Given the result of Equation 11 we see that our Adafruit LiPo battery exceeds our specification of an at least one-hour battery life.

Failures and Adjustments

As with all complex processes, we ran into failures along the way and had to make adjustments, the most significant of which involving our angle sensor. We had initially decided on using a hall effect encoder since it originally had the highest score in our Pugh chart (Table 7, which has since been updated) and we had a group member with a lot of familiarity with it. However, after feedback on our presentation about potential magnetic interferences (paired with some preliminary research into the issue), we decided to select another option that carried less risk of data distortion.

This led us to move onto an angular potentiometer. It had previously had the second highest rating on our Pugh chart, another team member had some familiarity with them, and the integration into our mechanism seemed pretty straight forward. However, upon preforming the error calculations for Design Driver 1, we had to eliminate that sensor as well, as we realized we hadn't considered all of the relevant errors and thus couldn't find one that met the spec while still being reasonably priced.

We then moved on to our last remaining option, the optical encoder, and upon searching for the ideal candidate, discovered a sensor that we had originally let fall to the wayside during our initial brainstorming phase: a capacitive sensor. We then started to analyze this option more heavily, and found it was a better fit than any of our other options on several accounts, including total error and compactness. Thus, we made the appropriate updates to our Pugh chart and analysis and have decided to use this sensor as our final selection.

When generating and evaluating concepts, the team decided that it would be advantageous to provide a means to detach and reattach at least one of the end links. This would allow for the range of motion to be "shifted" to accommodate different human joints that bend in different ways than the shoulder, which has been the focus for this design. For example, the knee and elbow joints bend from straight to almost fully bent, but only in one direction. Changing the position and angle of the end link would better emulate the range of motion of these joints. However, in detail design it was found that there is a lack of potential attachment points that allow for this reattachment while also retaining the device's ease of manipulation. A secondary reason to integrate the detachable link would be to make the device smaller for portability purposes, but the device is already so small that portability is not expected to be a concern even in its fully extended state. Due to the problems and lack of benefits of the removable link, it was abandoned. Both links will be permanently attached to the joint.

Low-Fidelity Prototyping

A low-fidelity prototype was constructed to increase understanding of the functionality of a universal joint as well as test the feasibility of achieving the desired range of motion. To construct the prototype, the following materials were used: cardboard, straws, toothpicks, and tape. We tried a couple different types of cardboard and found that corrugated cardboard worked well because the toothpicks could be placed between the layers. The cross design of the universal joint was achieved by cutting a hole through one straw for the other straw to go through and by placing one toothpick through the center of one straw direction and attaching a toothpick to the outside of the straw in the perpendicular direction. The third degree of freedom, the pivot joint, was made by sticking a toothpick into the end of one of the U-brackets, which allowed for rotation of the whole universal joint. Fig. 10 shows the full low-fidelity prototype, as well as the details for the three joint constructions.

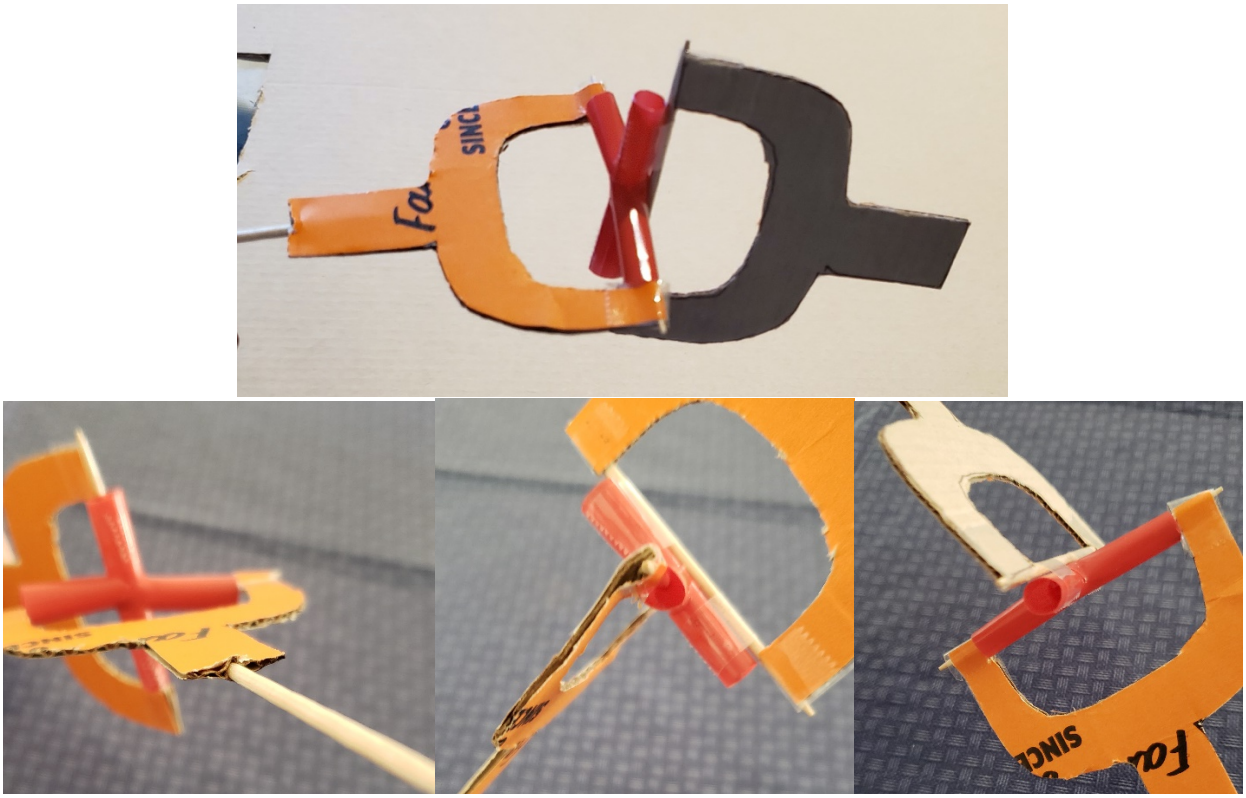

Fig. 10. Full view of the low-fidelity prototype used to simulate the motion of our joint design (top). The pivot joint (left) and the universal joint (middle, right) were modelled using toothpicks and straws connected to cardboard using tape.

Risk Assessment

To assess potential failures in our design, we performed a Failure Modes and Effects Analysis (FMEA). A table outlining the FMEA can be found in Appendix C. There were three key metrics assigned to potential failures: (1) Severity – how large the consequence of the failure mode is, (2) Occurrence – how likely is the failure mode to occur, and (3) Detection – how capable are current design controls of detecting a failure mode. A ranking between 1-5 is assigned for each of these metrics and the product of all three is reported as the final score for any given item. Typical FMEAs call this final output the Risk Priority Number (RPN).

The highest RPN of 20 belongs to battery over voltage failure which could result in a small fire as a worst-case scenario. Given the safety concern associated with this failure mode, we attempted to implement a backup detection system if both the embedded voltage protection circuit and the charging unit fails. Our original plan was to monitor the battery voltage using an analog input on the MCU and emit an obnoxious warning beep when battery voltage exceeds 4.2V. Unfortunately, our MCU's analog inputs cannot read inputs larger than 3.3V. This challenge could be overcome by using a voltage divider or op amp to lower the signal into a readable range, but we have not had time to implement and test these options. Although we failed to implement this warning beep, it is unlikely that both the overvoltage protection circuit and charger fail simultaneously, and the battery should be safe to charge if it is under constant supervision (which is recommended for all LiPo batteries regardless of the safety measures put in place).

The second highest RPN is 16 and that belongs to both the wiring harness failure and SD card failure. To mitigate risks associated with overwriting data on the SD card, we currently have two design controls in place. First, we wrote code to automate file naming and creation. This code generates a new CSV file every time the DAQ system is turned on and automatically generates a new filename by incrementing a file index number. Second, we simply oversized the SD card capacity at 8Gb to increase the time our device can be used prior to overwriting data. Admittedly, neither of these controls alert the user to when storage is full, instead we rely on the user to be aware of the status of their SD card. To make our DAQ more robust, we could add a storage full warning system by adding a blinking LED or a beeping noise to indicate that storage is full. We could even implement a cloud data storage system, so that whenever the user has access to the internet, data on the SD card will be moved to a cloud drive and free up space on the SD card as much as possible.

To mitigate risks associated with wiring harness failure, we have two design controls in place. First, we utilize stranded wires as opposed to solid core to increase flexibility. Second, we use multiple methods of strain relief including zip ties, heat shrink and hot glue near connectors. To further mitigate wire failure, we could use wire protecting covers, or even upgrade our encoders to make the device fully wireless. Further detail regarding design considerations for wire routing can be found in the DAQ section on pages 39-40.

Final Solution

After fully defining our design choices, we created a CAD model of our apparatus in SolidWorks. We've detailed the different sections with pictures throughout this section.

Full System

Due to the reasons listed in the previous sections, the Universal joint with an additional pivot joint was selected as our final joint design. An overall view of our prototype joint design with balloon callout is shown below in Figure 11

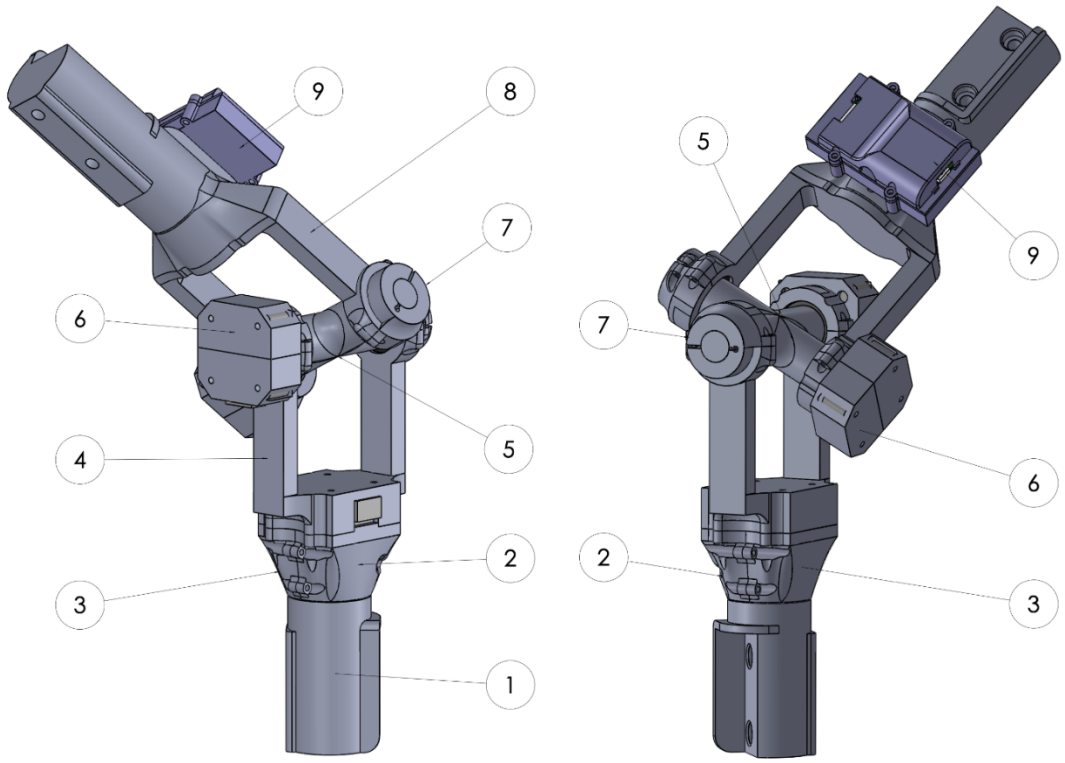

Fig. 11. Front view of our prototype joint design (left) and back view of our prototype joint design (right)

To clarify which part we are referring to in future sections, names of different parts are listed below:

1. Lower end link
2. End link front bearing cover
3. End link rear bearing cover
4. Lower U-brackets with sensor box and bearing case
5. Cross member
6. Cross member sensor box cover
7. Cross member bearing cover
8. Upper end link with upper U-brackets
9. Electronic box

Joint Design

In order to have 3 degrees of freedom, our joint design includes two types of joints: a universal joint, and a pivot joint. Figure 12 below shows the detailed view of the universal joint. Most of the minimum allowable dimensions for the universal joint were set based on the sensor dimensions, as the sensors are the most likely to cause interference and hence reduce the range of motion of the joint. In comparison, most of the maximum allowable dimensions for the universal joint were set based on Requirement 6, our portability requirement.

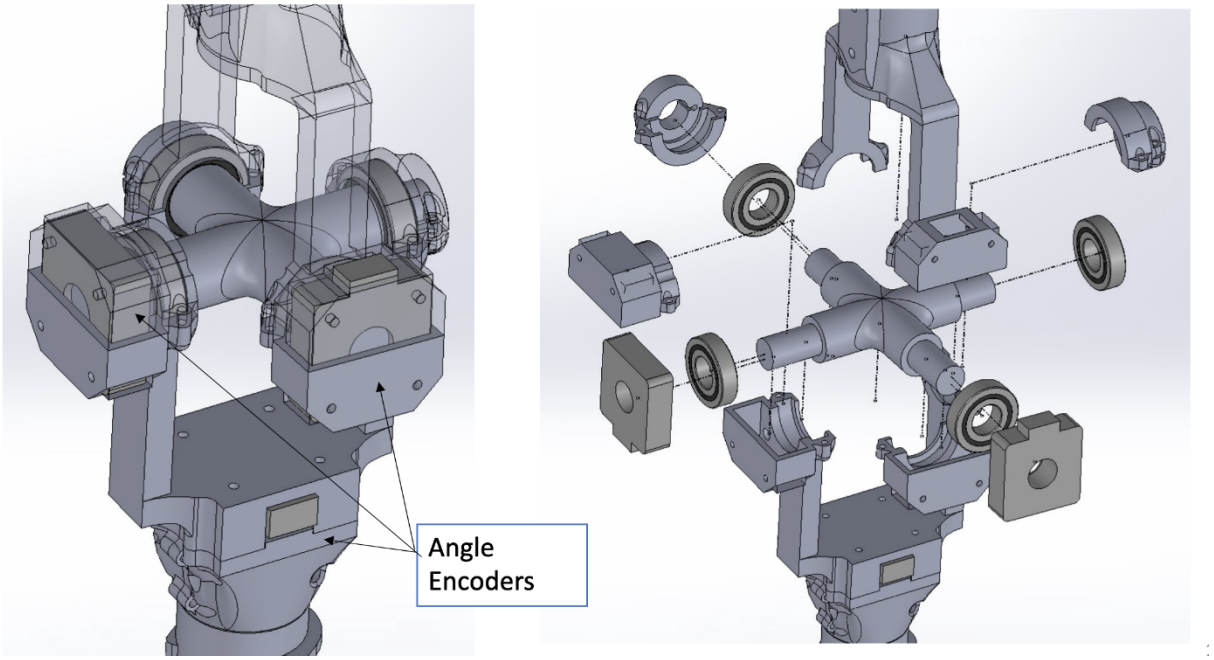

Fig. 12. Assembled view of the universal joint (left), exploded view of the universal joint (right)

As shown in Figure 12, the universal joint is made of a cross member connected to two U-brackets which continue on to become the end-link. To create rotation along both axis of the cross, four deep-grove ball bearings were used: two bearings on each end of both rotating axles. They were chosen according to Requirement #1 (measure Euler angles of links to within ± 1 degree) so we want to minimize play in the joint while providing a smooth and effortless operating experience. These types of bearing were chosen because within our design and the use case of this joint, those bearings will not undergo any substantial axial load, and their life span are longer than the designed life span of the system.

Our third degree of freedom is created through a pivot joint which can be seen below in Figure 13.

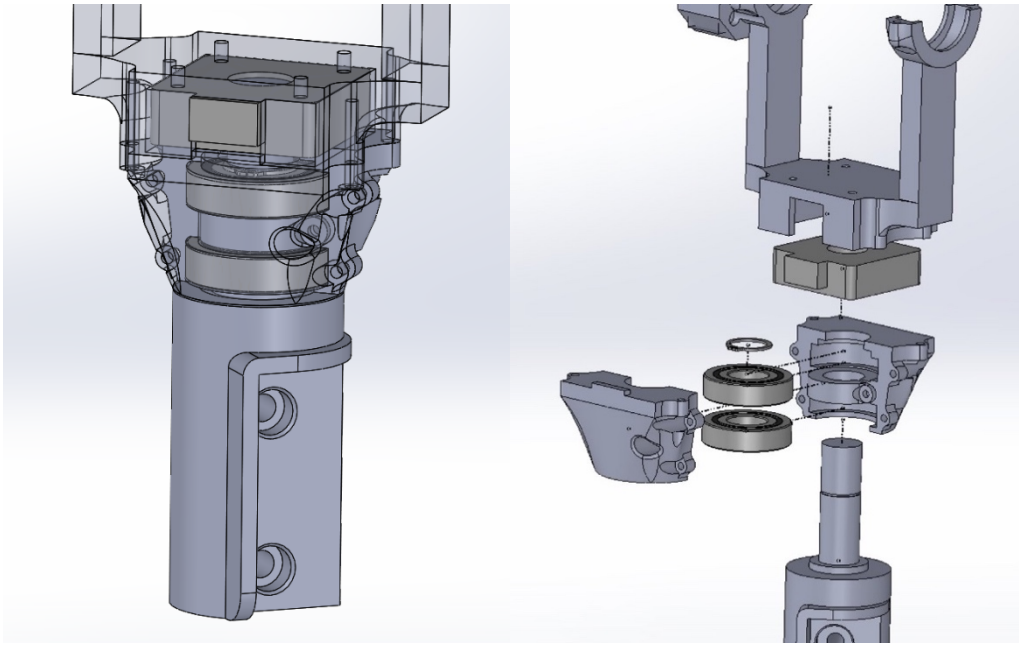

Fig. 13. Assembled view of the pivot joint (left) and an exploded view of the pivot joint (right)

This joint is composed of a U-bracket and one of the end links, and is created using the same bearing described above.

Sensor Integration

A good sensor integration design assures high accuracy of the output data, whereas a poorly designed sensor integration system could drastically increase error. Figure 14 shows the detailed CAD of the capacitive sensor we decided to use.

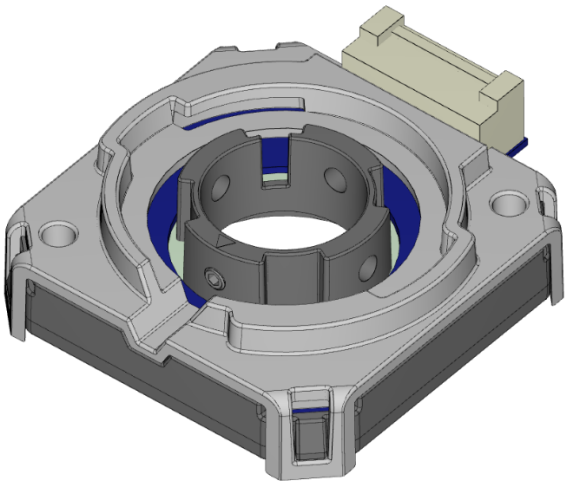

Fig. 14. Detailed CAD for AMT33 series capacitive angle encoder.

We designed the sensor integration mechanism so that it minimizes the number of intermediate components, ensures ease of assembly, and has high durability. Detailed views of the universal joint sensor integration design and pivot joint sensor integration design is shown and highlighted in Figure 15.

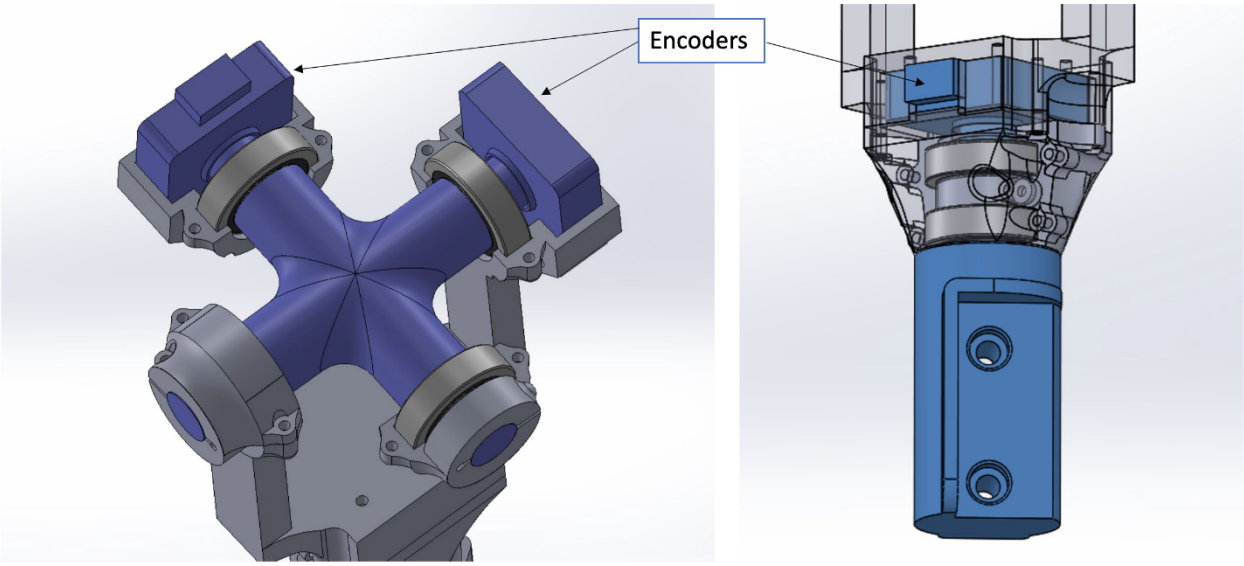

Fig. 15. Universal joint (left) and pivot joint (right) sensor integration

As shown in the right of Figure 15, there is a hollow shaft at the center of the sensor as a connection interface for the rotating axles. The end cross member was designed to have the same outer diameter as the inner diameter of the sensor to ensure a no-play connection. After all four bearings are installed on the cross member, two sensors can be pressed onto the ends of the cross member and secured with set screws. Since the sensor allows for off-centered operation, the alignment is not important as long as there's no slippage between the shaft and the encoder. Then the cross-bearing-sensor subassembly will be installed to both end links. This way, while the shaft of the sensor rotates with cross member, the rotational movement of end links can be transferred to the outer case of the sensor, and the relative angle is measured.

As shown in the left of Figure 15 above, the design is similar to that of the universal joint. However, this time, two bearings were first installed inside their designed groove. The shaft will then go through both bearings together. A snap ring will then install on the other end to ensure the shaft will not fall out of the bearings. The sensor will sit in the sensor box and be secured with screws.

Degree of Freedom Locking

Degree of freedom locking was required so that the mechanical joint can mimic different human joints. The design of the DoF-locking mechanism of the universal joint was shown and highlighted in Figure 16 below:

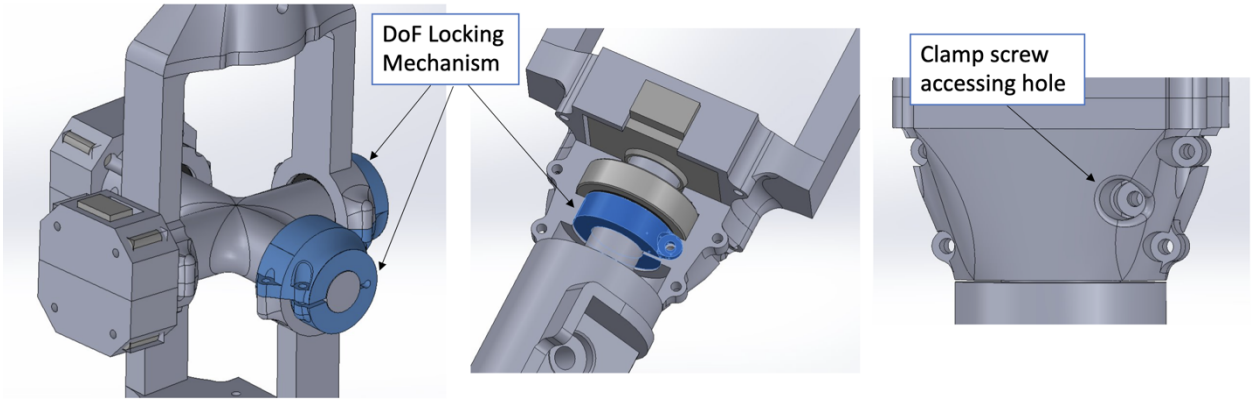

Fig. 16. DoF-locking mechanism for the universal joint (left), pivot joint (mid), and clamp screw accessing hole (right)

As shown in the left of Figure 16 above, for the universal joint, the DoF-locking mechanism, the clamp, was integrated together with bearing housing cap. After the cap has been tighten to the bearing case on the U-bracket with screws, the user could use the clamp screw to close or open the clamp. This way, the degree of freedom of the corresponding axis can be disabled by tightening or enabled by loosening the clamp screw.

For the pivot joint, the design is a bit more complicated, the clamp was put in between two end link bearings and was enclosed inside the cover. It was designed as such mainly due to two reasons: the stability of the end link relative to the fork, and the structural soundness of the joint. To ensure the stability of the end link, two ball bearings are separated as far as possible within the limited space. To ensure the structure soundness of the joint, the enclosed clamping mechanism was designed, so that the upper and the lower bearing case could both be load bearing structures. The upper bearing case goes over the clamp and two bearings, and has a clamp accessing hole, as shown in Figure 16, to lock or unlock this DoF.

End Link Design

PLA

Two primary advantages drove the selection of PLA (Polylactic Acid), a commonly 3D-printed thermoplastic, as a material for the end links: density and manufacturability. PLA is less dense than most other commonly used construction materials, and therefore it presents an opportunity to reduce weight. Due to the constraints on in-person contact this semester, machine shop availability has been questionable. In order to avoid problems with machine shop availability, the material selection was also made based on ease of manufacturing and the ability to avoid manual machining. The clear selection on that basis was to use PLA. Choosing to 3D print much of the design also allowed for complex geometries to be integrated into the design, much more so than would be possible using manual machining.

IMU Datum

To satisfy Requirement 10, datum geometry for IMU mounting was integrated into the end links. This geometry consists of three planar surfaces at right angles, as shown in Figure 17.

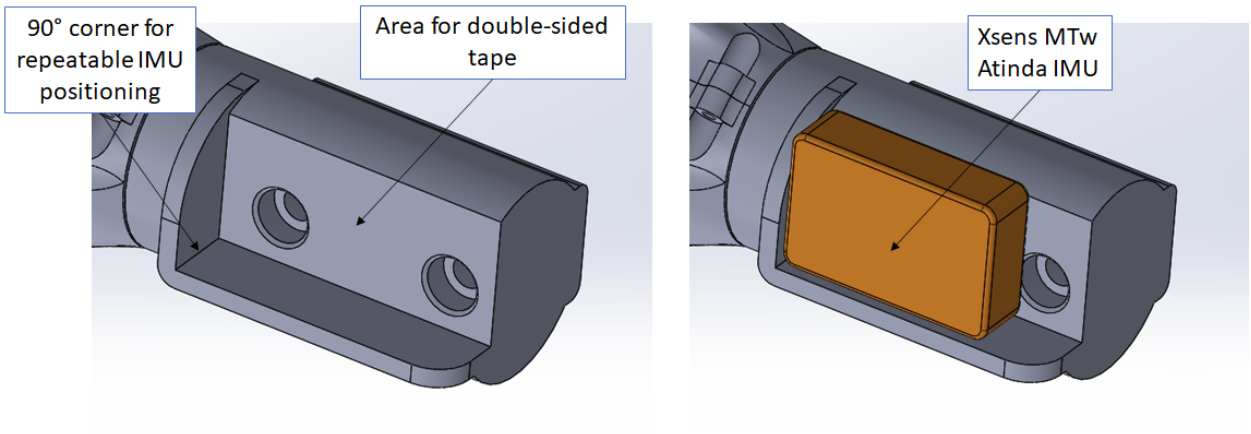

Fig. 17. IMU attachment geometry allows for precise, repeatable, and secure placement of IMUs on the end link. Multiple attachment methods are available to accommodate different IMU designs (left). An example IMU [71] provided by the sponsor fits comfortably within the attachment geometry (right).

The three datum planes produced by the end link geometry allow for repeatable IMU location, as the casing of most IMU sensor packages have mutually perpendicular sides which can be made coincident with the planes. Additionally, significant area has been left on the largest surface for double-sided tape which will securely attach the IMU.

Requirement 10 denotes a maximum deviation between the IMU attachment orientation and the axis of rotation of the link. Required dimensional accuracy can be determined from this maximum angular deviation and the length of the mounting surface or shaft. However, since FDM 3D printers (the kind that print in PLA) are somewhat variable in their dimensional accuracies depending on the brand, price point, and calibration quality, it is impossible to find a good estimate for dimensional accuracy to compare with the required tolerances of the part. Because of this, alignment will be ensured through verification tests. If it is found that the angular deviation does not satisfy Requirement 10, production of the end links may need to be outsourced to a firm with higher-accuracy 3D printing technology, such as SLA.

Rigid Body Clamp

To satisfy Requirement 12, an optional clamp was added to the design which is able to interface with the mounting holes on the end links. A diagram of the clamp is shown in Figure 18.

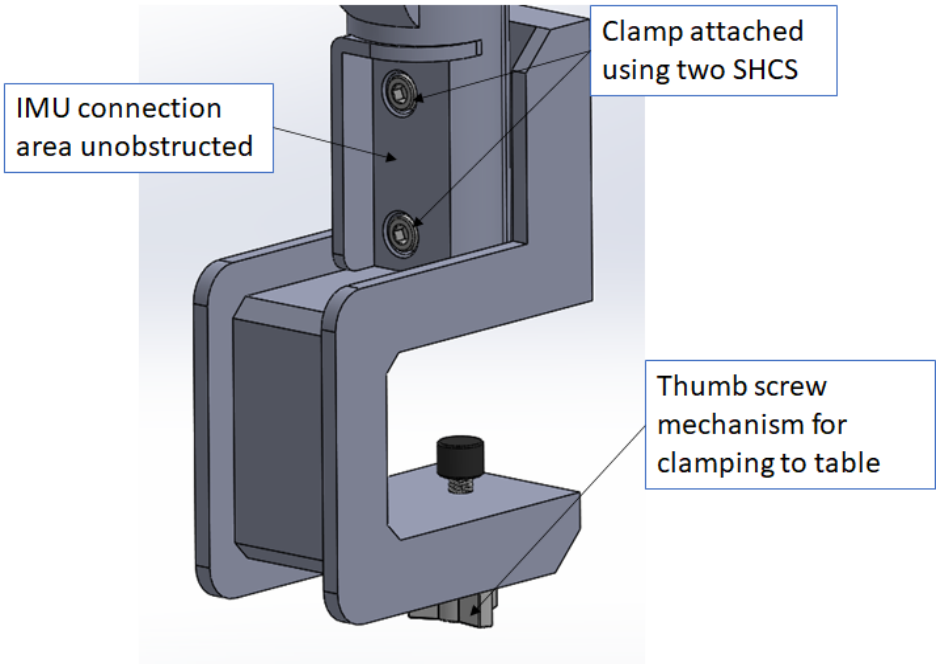

Fig. 18. A diagram of the mounting clamp devised for securely mounting the device to a rigid body.

To attach the device to a table, the clamp can be attached using two socket head cap screws. The mouth of the clamp can then be slid over the edge of a table or work bench, and then the thumb screw can be tightened. A plastic cap was added to the end of the thumb screw to avoid damaging the table in the case of overtightening.

Data Acquisition

Our data acquisition (DAQ) system consists of three primary components: (1) angle sensors, (2) a battery power supply (3) and a microcontroller unit (MCU) with a built in SD card slot. The angle sensors we chose for our application are CUI capacitive encoders which have been discussed at length on pgs. 20-21 and 29-31. The battery we selected for our device is a 4.4Wh lithium polymer battery sold by Adafruit. Battery selection and calculations can be found on pg. 31. The MCU we selected for our design is the PJRC Teensy 3.5. This small yet powerful device was chosen because it possesses the following features:

- Extremely small form factor
    - Dimensions: 62.3mm x 18.0mm x 4.2mm
    - Weight: 4.8g
- Built in SD card slot with SPI libraries for data logging
- Adequate number of 5V tolerant I/O pins for quadrature decoding
- Ability to conveniently add LiPo battery charger shield directly on top of board

In addition to these three primary components, a voltage booster was also required to allow our LiPo battery (nominally 3.7V) to provide 5V to the encoders. A block diagram displaying how these components interface is shown below in Figure 19.

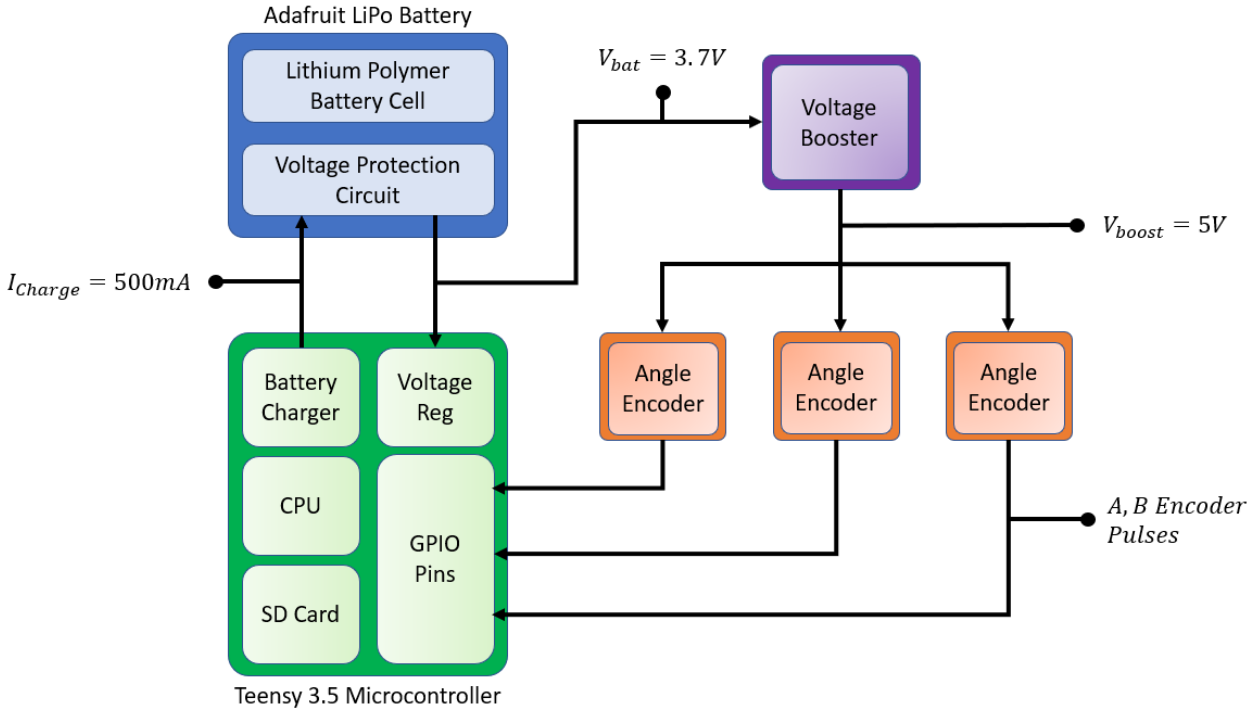

Fig. 19. Electrical block diagram for data acquisition system.

Due to the dynamic nature of this device, wire routing in the DAQ system was of significant concern. It was important to route the wires to the encoders such that the wires were never strained or tightly twisted by the motion of the joints, as this could cause the wires to unplug or be damaged. Figure 20 shows the planned wire routing paths for each encoder back to the microcontroller.

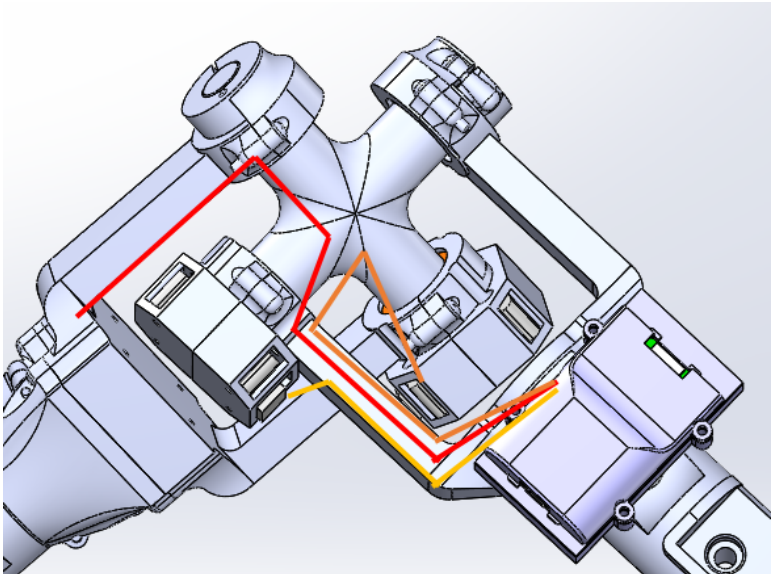

Fig. 20. Wire routing plan for power and data lines to the encoders.

This path eliminates twisting and tangling by minimizing the length of the wires that is free to move. When the wires are properly secured, only short lengths of the wires around the joints will be able to move. Since the device has predictable range of motion in these areas, it will be trivial to allow enough slack in these areas for full movement of the device without straining, while also minimizing the size of the tangle-prone wire loops.

Creation

Manufacturing Plan

For many of our mechanical parts, we plan to rely almost entirely on 3D printing for manufacturing. By utilizing a 3D printer owned by one of our team members, we will print out our pieces based off of our CAD model. Our CAD parts were modelled to include 3D printing tolerances. Sanding will be used to enhance the finish of the parts and adjust for any minor fit issues that could potentially arise in assembly. Additional mechanical components such as bearings and retaining rings have been purchased from McMaster Carr. For our electrical components, we do not have the expertise that would be required to design our own devices, so we have ordered and received pre-made components from Digi-Key. For the first prototype, the DAQ will be assembled on a "proto" PCB board from Adafruit. Once our 3D printed pieces are completed, we will begin integrating our electrical and mechanical components according to our main CAD assembly model.

Cost Assessment

For this project, Dr. Cain has approved a budget of $400. Appendix C shows the bill of materials used for this project. It is broken up into electrical components and mechanical components. The most expensive electrical components include three capacitive sensors for recording joint angles and wiring harnesses. The most expensive mechanical component is the PLA material that will be used for 3D printing. This is a rough estimate at this point, as we have yet to actually print any pieces. The final cost of all of the components was $408.32, which is slightly over budget for the project.

Verification

Verification tests have been created for each engineering specification and are currently in the process of being completed. A complete table outlining tests for all specifications as well as their completion status can be found in Appendix D. The remainder of this section will focus on describing verification tests associated with our three design drivers as well as any of the other more complicated tests that warrant more discussion.

Design Driver 1: Total Error

Being able to measure Euler angles within ± 1° (Spec 1), will be verified by comparing our capacitive sensor's angular output to a Medigauge digital goniometer, which have reported accuracies of ± 0.2°. and ± 0.5° respectively. While the goniometer measurement does have a lower accuracy than our encoder, it is able to resolve angles smaller than our spec of ± 1°. To perform this test, we will rigidly attach the main shaft of the goniometer to the encoder hub with a set screw. We will then mount the encoder and goniometer in a 3D printed fixture which will fix the encoder housing and one end of the goniometer in place (see Figure 21 below).

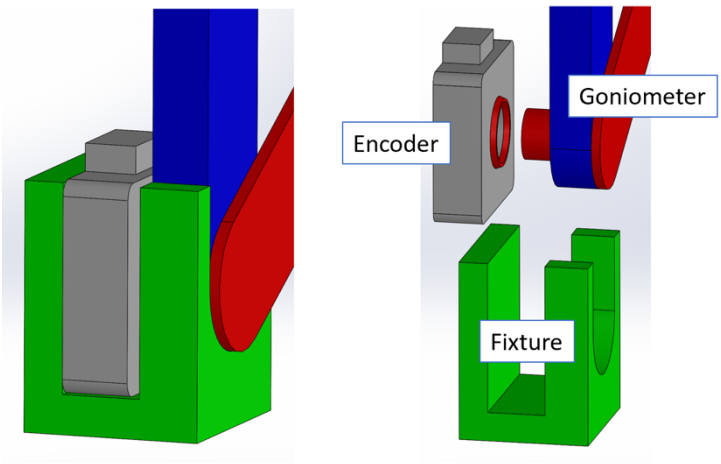

Fig. 21. Goniometer Test Fixture

Once setup, we will simply move the goniometer through different angles while outputting encoder data to our serial monitor and ensure they are within ± 1° (see Equation 12 below).

$$\theta_{gon} \pm 0.5° - \theta_{enc} \leq \pm 1° \tag{12}$$

If the inequality in Equation 12 is satisfied, we can be confident that our encoders are providing sufficiently accurate angles. Note that the reported encoder accuracy of ± 0.2° is not included in the above equation because this is what we are measuring. In other words, if the goniometer measurement were perfect and the encoder accuracy error was exactly as reported on its datasheet then Equation 13 would hold

$$\theta_{gon} - \theta_{enc} \cong \pm 0.2° \tag{13}$$

Design Driver 2: Range of Motion

As part of the verification process, the shell of the device was printed and assembled. An image of the assembled shell is shown in Figure 22:

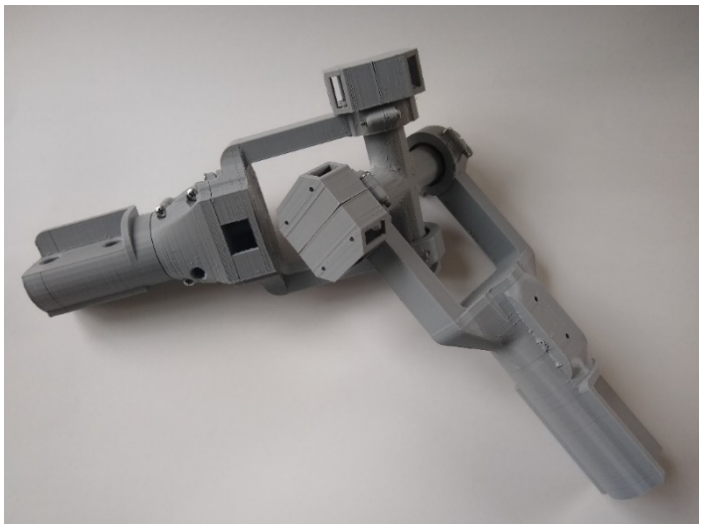

Fig. 22. The mechanical shell of the device was used to verify it with respect to the range-of-motion requirement.

To verify that the device can move through the required range of motion of 180 degrees in all three axes, a protractor was used while manipulating the device to sweep through its full range of motion. Before starting the test, convenient edges on each side of each joint were selected to use as references for the angle measurement. At the extremes of the range of motion for each joint, the angle measurement between the selected reference edges from the protractor was recorded. Subtracting the angle measurements at the limits of motion yielded the range of motion of each joint. For both hinge joints in the universal joint, the range of motion was determined to be 252 degrees, and the pivot joint can rotate indefinitely in either direction. Therefore, the device satisfies the range of motion requirement.

Design Driver 3: Battery Life

For verifying the achievable battery life for our selected battery, testing was straight forward. All the electrical components that are used in the apparatus were connected to the battery and turned on. A timer was started to see how long the battery could power the electrical components. The battery was able to meet our specification of lasting for at least one hour. We continued the testing to try and determine the full battery lift of one charge but had to stop the test after 5 hours due to time limitations on our verification testing and maintain safe-use practices and not leave the components on while unattended to.

Sampling Rate

Another key specification is that our DAQ system sample at a rate greater than 60Hz (Spec 7). To verify this, we used a basic timer function to measure the rate at which our code executes. Although this check is trivial to perform, it has been included in this section due to the mixed results we saw during initial testing. Excluding any writing to the SD card, we achieved a sampling rate of approximately 10kHz. When including datalogging to the SD card we achieved a sampling rate of roughly 300Hz. This large slowdown is to be expected due to the latency involved with writing to the SD card, but still passes our 60Hz specification. Unfortunately, writing to the SD card also exhibited sporadic loop times that were greater than 0.2s (less than 5Hz). This was most likely an artifact of the Teensy “dumping” a large internal buffer of data to the SD card, and it remains to be seen whether this can be avoided. Future testing and code optimization will be performed to attempt to mitigate this problem.

Magnetic Interference

The last specification worthy of discussion in this section is Specification 7, stating that no materials in the mechanism can change the magnetometer reading by > 0.1%. This will be verified using a fixture similar to the one used for Design Driver 1 verification, as shown in Figure 21. In this experiment, the fixture would be adjusted such that the whole gimbal assembly can be installed onto the fixture and is capable of locking two degrees of freedom of the gimbal to only allow the gimbal to freely rotates along one axis where the goniometer is attached. Starting from 0° mark, the gimbal will be moved to the 180° mark and back to 0° to mimic two full 180° travel forward and backward. At each 5°-mark, magnetometer data was exported from IMU and recorded. For the second run, the gimbal was uninstalled and only the IMU was installed onto the fixture. The fixture would be designed such that the IMU can be installed at the same location as it is on the gimbal. All other procedures are identical to the first run. The two sets of data can them be compared to ensure the change in the IMU measurement stays within 0.1%.

Discussion and Recommendations

Currently, we feel like our apparatus design has the potential to be successful, but we are unable to make definite conclusions about it because we were not able to complete all of our verification methods within the time frame of this course. Our Tier 1 specifications indicated the project specifications that were most important for us to achieve baseline functionality of our device, and we have five out of eight of these specifications completed successfully with the remaining three still in progress. Our verification table in Appendix D shows which specifications are completed. However, in addition to having some of our specifications successfully completed for our first-iteration physical prototype, we experienced a couple functionality failures in our device.

One of the failures of our design occurred in the degree-of-freedom locking mechanism. Since both the shaft and the clamp are made of PLA, which has a relatively high level of compliance when compared with other commonly used structural materials, the clamp was unable to achieve the necessary amount of clamping force. This fact combined with the low friction coefficient between PLA parts results in clamping mechanisms that are unable to constrain motion effectively. One way to fix this problem would be to use the parts as designed but manufacture the clamps and shafts from a metal, such as aluminum. This would retain all of the functionality of the current design, including the ability to lock at any angle, but would make manufacturing much more difficult. Another possibility would be to change the fundamental concept of the locking mechanism to something that would not be affected by the mechanical shortcomings of PLA. For example, the pin concept that was generated during the concept exploration phase may be more effective in this way. In general, the degree of freedom locking system is not a Tier 1 specification that is critical to basic functionality, so for this first iteration prototype, this specification will not be met.

An additional shortcoming of the design was the shaft for our pivot joint. This shaft held the two bearings that allowed for rotation of the shaft. This setup is shown in Fig. 13 in the Joint Design subsection of the Final Solution section above. To give the bottom bearing a level, flat surface to set on, no fillet was added on the CAD model between the shaft and its base, which can be seen in Fig. 22 below. This sharp corner created an area of concentrated stress. While we were testing the functionality of the device, the PLA shaft cracked at this point of concentrated stress. To address this failure, we generated a second iteration of this specific part. For a second iteration of this part, the CAD model has been modified to include a small fillet between the shaft and its base, as well as a circular cut through the shaft where a quarter inch brass shaft will be press fit to relieve some of the load from the PLA shaft. (Brass was chosen purely out of convenience based on what material we had immediate access to. Other metals such as aluminum or steel would've also been valid choices.) Additionally, a small chamfer has been added to the top of the shaft for ease of insertion of the brass shaft. The modified CAD model is also shown in Fig. 23.

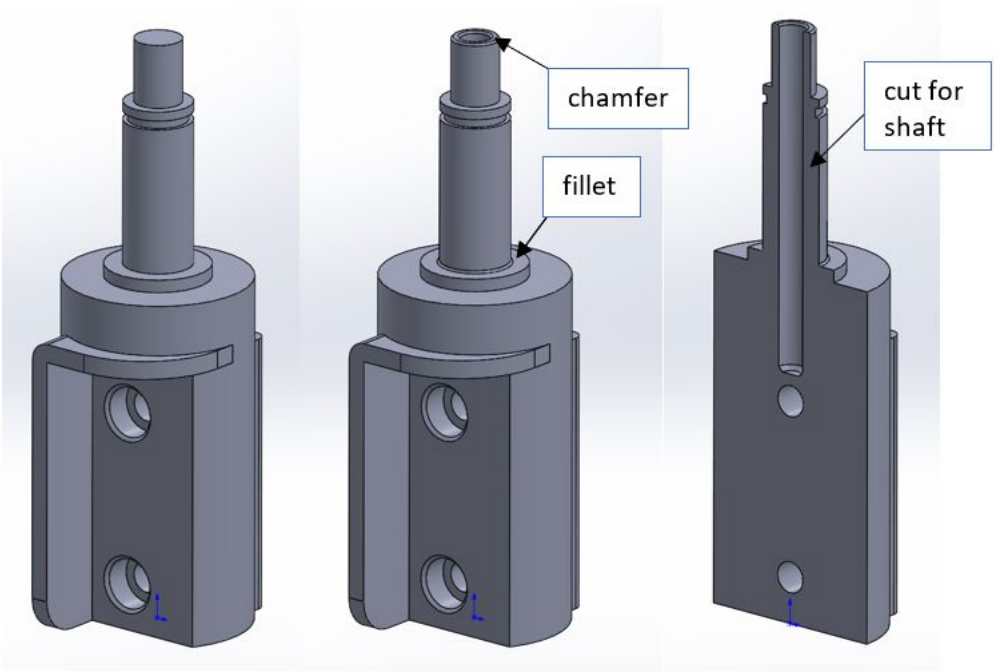

Fig. 23. The CAD models for the original pivot joint shaft (left) and for the modified pivot joint shaft with the fillet and chamfer addition (middle) and the cut for metal shaft addition (right).

Going forward, we plan to 3D print the second iteration of the pivot joint shaft and complete the remaining verification tests for the Tier 1 specifications. If any components begin to fail, we will use the 'Recommended Actions' from our FMEA assessment to determine the necessary steps that need to be made to ensure functionality of our device. Our intention is to be able to give our stakeholder, Dr. Cain, our physical prototype that meets at least all our Tier 1 specifications before the start of next semester.

One additional recommendation we have is for a non-portable method of use. Although our main idea is based on portability and being able to use a battery for power, an additional method of use would be to connect our system to a computer rather than a battery. The main advantage to this method is being able to watch the serial monitor in real time instead of collecting data on the SD card and having to look at it after the collection is completed. This non-portable method could be especially helpful to Dr. Cain to quickly validate that the sensors are reading properly before starting a long data collection test.

Conclusion

Many biomechanical fields benefit from the collection of accurate joint angle data. Due to their small size and low cost, Inertial Measurement Units (IMUs) have become very popular sensors for this application. However, producing accurate joint angles from IMU data is not trivial. One of the issues with the IMU data is that the IMU-reported positions and orientations are susceptible to drift over time because of the iterative process used in IMU data collection. Our task was to produce a portable device that provides reliable ground-truth joint angle data to validate algorithms that have been created to try and account for drift so that accurate joint angles can be acquired from IMU data.

To begin, a literature search was conducted to find any relevant information in the current body of scientific knowledge. Based on the information gathered and input from the stakeholder, requirements

and specifications for the apparatus were determined. Design concepts were then generated, and divergent thinking techniques were used to fully explore the design space. These concepts were then narrowed down to just a few top options which best fit the requirements and specifications before being narrowed down to a single option to move forward with.

Our final design selection is a universal joint with one end link being attached to a pivot joint and capacitive sensor to measures angles. One capacitive sensor is mounted along each of the three axes of rotation to record their positioning. Additionally, there are mounts on the end links for IMUs, so that data can be recorded for the apparatus motion by the angular sensors and the IMUs simultaneously.

We determined verification tests to check that each of our specifications could be fulfilled. Due to time restraints of the course, we were not able to complete all of our verification testing on our first-iteration prototype, but the methods to complete them have been outlined. FMEA analysis was also conducted to determine solutions for any component failure that may arise during further testing.

If we are able to continue verification of our device beyond the class so that it fulfills our requirements and specifications, we will give the device to Dr. Cain. He will then be able to use our device and be better equipped to develop and validate IMU joint algorithms for his use cases, such as for studying the mechanics of arm movements of wheelchair-bound individuals. In the broader context of the wider research community, a device like this may make the acquisition of joint angles cheaper, easier, and more accurate for everyone. The device will allow researchers on a low budget, with time constraints, or without access to motion capture systems the opportunity to develop and validate IMU joint angle algorithms for their specific use cases. This in turn makes it much less expensive and cumbersome to perform experiments, because the IMUs can then be used for data acquisition instead of more expensive and bulky equipment. When research involving joint angles becomes easier and cheaper, faster progress will be made towards helping people with all kinds of conditions and injuries.

Acknowledgements

We owe much of our success to the following individuals who gave us the information, capabilities, and tools we needed to be successful this semester.

Dr. Noel Perkins	Our dear professor who gave us timely, useful feedback, and provided direction when we needed it.
Dr. Stephen Cain	Our stakeholder whose vision made this whole project possible.
Joanna Thielen	Our librarian who helped us find the best information we could, as efficiently as possible.
Heather Cooper	Our lecturer who provided us with information through the learning blocks which helped us throughout all aspects of the project.

Authors

Isaac Harris
isharris@umich.edu
734-680-5693

Primary Role: Stakeholder Point of Contact

Isaac Harris is from Pinckney, MI and is pursuing a master's degree in mechanical engineering with a concentration in controls and robotics. He is passionate about biomechanics research and currently works as a research assistant for the UM Neurobionics Lab where he develops robotic prostheses. In his free time, Isaac enjoys spending time with his wife and two baby daughters, playing disc golf, and tinkering with electronics.

Chelsea Nienhuis
chelnien@umich.edu
(616) 953-9277

Primary Role: Co-Record Manager

Chelsea Nienhuis is from Zeeland, MI and is a senior pursuing a degree in mechanical engineering. Following graduation, she plans to work at Koops Automation Systems in Holland, MI as a controls engineer. Outside of classes at UM, she enjoys competing in intramural sports such as basketball, volleyball, football, and ultimate frisbee (during past non-COVID semesters) and being involved with her church on campus.

Alex Rees
avrees@umich.edu
(616) 368-1164

Primary Role: Facilitator

Alex Rees is pursuing a degree in mechanical engineering with a minor in business from the University of Michigan and plans to pursue a masters in energy and materials following graduation. Outside of classes he's a president of the organization that runs blood drives on campus and enjoys being able to make an impact in the world around him.

Keyen Yockey
yockeyke@umich.edu
(734) 249-4333

Primary Role: Accountant

Keyen Yockey is from Ann Arbor, MI, and is pursuing a degree in mechanical engineering with a minor in computer science. He has been interested in mechanical engineering since joining an FRC team in high school, where he was a lead on both design and fabrication. He now enjoys developing VTOL aircraft as a structural design lead on the student project team Michigan Vertical Flight Technology. He plans on pursuing a master's degree in robotics after graduation.

Ziqi Wang

ziqiw@umich.edu

(617)309-9097

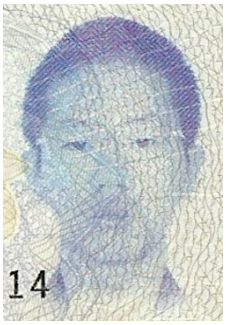

Primary Role: Co-Record Manager

Ziqi Wang is from Beijing, China, and is pursuing dual degree in mechanical engineering and in computer science. After graduation, his plan is to keep pursing a Ph.D. in mechanical engineering. Outside of classes, he loves snowboarding, scuba diving, and free diving. He hates taking selfies of any kind.

Citations

[1] A. Maximilian, W. Kilian, S. Franz, and D. Sebastian, "Implementation and validation of human kinematics measured using IMUs for musculoskeletal simulations by the evaluation of joint reaction forces," 2017, doi: 10.1007/978-981-10-4166-2_31.

[2] H. Zhou and H. Hu, "Human motion tracking for rehabilitation-A survey," *Biomed. Signal Process. Control*, vol. 3, no. 1, pp. 1–18, 2008, doi: 10.1016/j.bspc.2007.09.001.

[3] H. H. C. M. Savelberg, M. A. T. M. Vorstenbosch, E. H. Kamman, J. G. W. Van De Weijer, and H. C. Schambardt, "Intra-stride belt-speed variation affects treadmill locomotion," *Gait Posture*, vol. 7, no. 1, pp. 26–34, 1998, doi: 10.1016/S0966-6362(97)00023-4.

[4] C. A. Clermont, L. C. Benson, W. B. Edwards, B. A. Hettinga, and R. Ferber, "New considerations for wearable technology data: Changes in running biomechanics during a marathon," *J. Appl. Biomech.*, vol. 35, no. 6, pp. 401–409, 2019, doi: 10.1123/jab.2018-0453.

[5] G. Pendharkar, P. Percival, D. Morgan, and D. Lai, "Automated method to distinguish toe walking strides from normal strides in the gait of idiopathic toe walking children from heel accelerometry data," *Gait Posture*, vol. 35, no. 3, pp. 478–482, 2012, doi: 10.1016/j.gaitpost.2011.11.011.

[6] J. H. Kim and K. H. Sienko, "The design of a cell-phone based balance-training device," *J. Med. Devices, Trans. ASME*, vol. 3, no. 2, pp. 1–1, 2009, doi: 10.1115/1.3135151.

[7] M. C. Cirstea and M. F. Levin, "Improvement of arm movement patterns and endpoint control depends on type of feedback during practice in stroke survivors," *Neurorehabil. Neural Repair*, 2007, doi: 10.1177/1545968306298414.

[8] D. Roetenberg, H. Luinge, and P. Slycke, "Xsens MVN: full 6DOF human motion tracking using miniature inertial sensors," *Xsens Motion Technol. BV, …*, 2009.

[9] E. Foxlin and M. Harrington, "WearTrack: a self-referenced head and hand tracker for wearable computers and portable VR," *Int. Symp. Wearable Comput. Dig. Pap.*, 2000, doi: 10.1109/iswc.2000.888482.

[10] Y. Tian, X. Meng, D. Tao, D. Liu, and C. Feng, "Upper limb motion tracking with the integration of IMU and Kinect," *Neurocomputing*, vol. 159, no. 1, pp. 207–218, 2015, doi: 10.1016/j.neucom.2015.01.071.

[11] D. H., J. B.M., and A. K., "A new approach to accurate measurement of uniaxial joint angles based on a combination of accelerometers and gyroscopes," *IEEE Trans. Biomed. Eng.*, 2005.

[12] X. Yun and E. R. Bachmann, "Design, implementation, and experimental results of a quaternion-based Kalman filter for human body motion tracking," *IEEE Trans. Robot.*, 2006, doi: 10.1109/TRO.2006.886270.

[13] R. S. McGinnis and N. C. Perkins, "A highly miniaturized, wireless inertial measurement unit for characterizing the dynamics of pitched baseballs and softballs," *Sensors (Switzerland)*, vol. 12, no. 9, pp. 11933–11945, 2012, doi: 10.3390/s120911933.

[14] T. Seel, J. Raisch, and T. Schauer, "IMU-based joint angle measurement for gait analysis," *Sensors (Switzerland)*, vol. 14, no. 4, pp. 6891–6909, 2014, doi: 10.3390/s140406891.

[15] O. J. Woodman, "An introduction to inertial navigation." Cambridge University, Cambridge, 2007, [Online]. Available: https://www.cl.cam.ac.uk/techreports/UCAM-CL-TR-696.pdf.

[16] E. C. Frick and E. C. Frick, "Mitigation of magnetic interference and compensation of bias drift in inertial sensors," 2015.

[17] J. Favre, B. M. Jolles, R. Aissaoui, and K. Aminian, "Ambulatory measurement of 3D knee joint angle," *J. Biomech*, vol. 41, pp. 1029–1035, 2008.

[18] K. J. O'Donovan, R. Kamnik, D. T. O'Keeffe, and G. M. Lyons, "An inertial and magnetic sensor based technique for joint angle measurement," *J. Biomech*, vol. 40, pp. 2604–2611, 2007.

[19] A. Brennan, J. Zhang, K. Deluzio, and Q. Li, “Quantification of inertial sensor-based 3D joint angle measurement accuracy using an instrumented gimbal,” *Gait Posture*, vol. 34, no. 3, pp. 320–323, 2011, doi: 10.1016/j.gaitpost.2011.05.018.
[20] A. Boresi, R. Schmidt, and F. Mei, *Engineering Mechanics: Dynamics*, vol. 54, no. 6. 2001.
[21] M. Suneja, J. F. Szot, R. F. LeBlond, and D. D. Brown, “The Spine, Pelvis, and Extremities,” in *DeGowin’s Diagnostic Examination, 11e*, New York, NY: McGraw Hill, 2020.
[22] D. A. Winter, *Biomechanics and Motor Control of Human Movement: Fourth Edition*. 2009.
[23] “XROMM: Hardware.” https://www.xromm.org/hardware/ (accessed Sep. 25, 2020).
[24] D. L. Miranda, J. B. Schwartz, A. C. Loomis, and E. L. Brainerd, “Static and Dynamic Error of a Biplanar Videoradiography System Using Marker-Based and Markerless Tracking Techniques,” *J. Biomech. Eng.*, vol. 133, no. 12, 2011, [Online]. Available: https://search.lib.umich.edu/articles/record/FETCH-LOGICAL-14392-a4fd465b34044d58b4e0762beb14303dc9974e1a2f644a5f92527d1682dba433.
[25] T. W. Lu and J. J. O’Connor, “Bone position estimation from skin marker co-ordinates using global optimisation with joint constraints,” *J. Biomech.*, vol. 32, no. 2, pp. 129–134, 1999, doi: 10.1016/S0021-9290(98)00158-4.
[26] E. S. Encoder, “Enc - a5si - 0050 - 394 - h - g,” no. 714. pp. 0–3.
[27] B. Diagram, “iC-MH 12,” pp. 1–23, 2008.
[28] C. Plastic, “NP24HS Series Single Turn Hollow Shaft Potentiometer NP24HS Series Single Turn Hollow Shaft Potentiometer,” pp. 2–3.
[29] S. Operation, I. Options, O. Are, and C. With, “8-Bit Analog-To-Digital Converters With Serial Control,” no. January 1995, pp. 1–12, 1996.
[30] “En DIGITAL CAMERA About This Manual.”
[31] “User Guide motog6.” Accessed: Sep. 28, 2020. [Online]. Available: https://ss7.vzw.com/is/content/VerizonWireless/Catalog Assets/Devices/Motorola/moto-g6/ug-moto-g6.pdf.
[32] “Getting Started with Arduino UNO | Arduino.” https://www.arduino.cc/en/Guide/ArduinoUno (accessed Sep. 28, 2020).
[33] “Transfer Files Between Your PC and Your Raspberry Pi.” https://www.dexterindustries.com/howto/how-to-transfer-files-to-your-raspberry-pi-from-a-pc-computer/ (accessed Sep. 28, 2020).
[34] “HP DeskJet 2600 All-in-One series.”
[35] “Siri Remote - Apple.” https://www.apple.com/shop/product/MQGD2LL/A/siri-remote (accessed Sep. 29, 2020).
[36] “Pixel 4a Hardware Specs - Google Store.” https://store.google.com/product/pixel_4a_specs (accessed Sep. 29, 2020).
[37] “Swingline Commercial Desktop Full Strip Stapler, 20 Sheet Capacity, Black at Staples.” https://www.staples.com/Swingline-Commercial-Desktop-Full-Strip-Stapler-20-Sheet-Capacity-Black/product_504308 (accessed Sep. 29, 2020).
[38] “2 Quart & 4 Quart Saucepans | Best Stainless Steel Saucepans.” https://madeincookware.com/products/stainless-steel-sauce-pan?variant=47127480714&utm_source=google&utm_medium=shopping&utm_campaign=1102 1698521-107486541305&utm_content=47127480714&audience=pros&gclid=CjwKCAjwkoz7BRBPEiwAeK w3q9SHQ5cARiKJMjEoUvHV21lm17CcD3riYnSMcONsQMp7wDNIvNfuTRoCFJIQAvD_BwE (accessed Sep. 29, 2020).
[39] “20V MAX* Lithium Drill/Driver - BDCDD120C | BLACK+DECKER.” https://www.blackanddecker.com/products/power-tools/portable-power-tools/drills/20v-max-

lithium-drilldriver/bdcdd120c (accessed Sep. 29, 2020).
[40] "20V MAX* XR® Li-Ion Brushless Compact Drill / Driver Kit - DCD791D2 | DEWALT." https://www.dewalt.com/products/power-tools/drills/drills-and-hammer-drills/20v-max-xr-liion-brushless-compact-drill--driver-kit/dcd791d2 (accessed Sep. 29, 2020).
[41] "7 Amp Blower - LB700 | BLACK+DECKER." https://www.blackanddecker.com/products/lawn-and-garden/lawn/leaf-blowers-and-sweepers/7-amp-blower/lb700 (accessed Sep. 29, 2020).
[42] "GT Revolution | 20V 12" String Trimmer & Lawn Edger | WORX." https://www.worx.com/20v-gt-revolution-cordless-string-trimmer-wg170-2.html?gclid=CjwKCAjwkoz7BRBPEiwAeKw3q_t2b0U1L448fJiNgrQsAzcLdDtBFXoE5jqfb6GvvFqJLe-Qgt_z3RoC_c4QAvD_BwE (accessed Sep. 29, 2020).
[43] "20V MAX Lithium 10 in Chainsaw - LCS1020B | BLACK+DECKER." https://www.blackanddecker.com/products/lawn-and-garden/trees-and-shrubs/woodcutting/20v-max-lithium-10-in-chainsaw/lcs1020b (accessed Sep. 29, 2020).
[44] "HERO7 Black Tech Specs." https://gopro.com/en/us/shop/hero7-black/tech-specs?pid=CHDHX-701-master (accessed Sep. 29, 2020).
[45] "iPhone 11 Pro - Technical Specifications - Apple." https://www.apple.com/iphone-11-pro/specs/ (accessed Sep. 29, 2020).
[46] "MacBook Pro 16-inch - Technical Specifications - Apple." https://www.apple.com/macbook-pro-16/specs/ (accessed Sep. 29, 2020).
[47] "Dell XPS 17 Laptop | Dell USA." https://www.dell.com/en-us/shop/dell-laptops/new-xps-17-touch-laptop/spd/xps-17-9700-laptop/xn9700cto220s#techspecs_section (accessed Sep. 29, 2020).
[48] "VariZoom VZZGRIG Video Camera & DSLR Supports." https://www.varizoom.com/product/vzzgrig/ (accessed Sep. 29, 2020).
[49] A. M. Koontz, R. A. Cooper, M. L. Boninger, A. L. Souza, and B. T. Fay, "Shoulder kinematics and kinetics during two speeds of wheelchair propulsion," *J. Rehabil. Res. Dev.*, vol. 39, no. 6, pp. 635–649, 2002.
[50] P. D. Neilson, "Speed of response or bandwidth of voluntary system controlling elbow position in intact man," *Med. Biol. Eng.*, vol. 10, no. 4, pp. 450–459, 1972, doi: 10.1007/BF02474193.
[51] U. H. Lee, C. W. Pan, and E. J. Rouse, "Empirical Characterization of a High-performance Exterior-rotor Type Brushless DC Motor and Drive," *IEEE Int. Conf. Intell. Robot. Syst.*, pp. 8018–8025, 2019, doi: 10.1109/IROS40897.2019.8967626.
[52] H. Pontzer, J. H. Holloway, D. A. Raichlen, and D. E. Lieberman, "Control and function of arm swing in human walking and running," *J. Exp. Biol.*, vol. 212, no. 4, pp. 523–534, 2009, doi: 10.1242/jeb.024927.
[53] K. Nagarchi, T. Jayachandra Pillai, S. H. Saheb, K. Brekeit, and M. Alharbi, "Morphometry of clavicle," *J. Pharm. Sci. Res.*, vol. 6, no. 2, pp. 112–114, 2014.
[54] G. Mall, M. Hubig, A. Büttner, J. Kuznik, R. Penning, and M. Graw, "Sex determination and estimation of stature from the long bones of the arm," *Forensic Sci. Int.*, 2001, doi: 10.1016/S0379-0738(00)00445-X.
[55] D. Nowka, M. Kok, and T. Seel, "On motions that allow for identification of hinge joint axes from kinematic constraints and 6D IMU data," *2019 18th Eur. Control Conf. ECC 2019*, pp. 4325–4331, 2019, doi: 10.23919/ECC.2019.8795846.
[56] J. Favre, R. Aissaoui, B. M. Jolles, J. A. de Guise, and K. Aminian, "Functional calibration procedure for 3D knee joint angle description using inertial sensors," *J. Biomech.*, vol. 42, no. 14, pp. 2330–2335, 2009, doi: 10.1016/j.jbiomech.2009.06.025.
[57] and R. G. Christian, J.L, S.R. Daly, S. Yilmaz, C. Seifert, "Design heuristic support two modes of idea generation: Initiating ideas and transitioning among concepts," *American Society for*

Engineering Education, 2012. https://www.designheuristics.com/ (accessed Oct. 19, 2020).
[58] "ENC-A5SI with Index - Optical Incremental Rotary." https://www.anaheimautomation.com/products/encoder/incremental-rotary-item.php?sID=352&serID=5&pt=i&tID=1054&cID=422 (accessed Oct. 08, 2020).
[59] E. Characteristics, P. Dimensions, and E. Characteristics, "6537/6538 – 22 mm Precision Potentiometer," 2015.
[60] S. Board, "Hall Effect Encoder," pp. 1–35, 2015.
[61] "Orbis™ true absolute rotary encoder - www.rls.si." https://www.rls.si/eng/orbis-true-absolute-rotary-encoder?partNumbers=BR10SPC14B12CD00 (accessed Oct. 08, 2020).
[62] C. Inc, "Series : Amt10 | Description : Modular Incremental Encoder," pp. 1–8, 2017, [Online]. Available: http://www.cui.com/product/resource/amt10-v.pdf.
[63] "Online Materials Information Resource - MatWeb." http://www.matweb.com/index.aspx (accessed Oct. 16, 2020).
[64] "Is PLA Recyclable? – Bioplastics News." https://bioplasticsnews.com/2020/04/05/is-pla-recyclable/ (accessed Oct. 16, 2020).
[65] "Why Should We Recycle Aluminum?" https://www.thoughtco.com/the-benefits-of-aluminum-recycling-1204138 (accessed Oct. 16, 2020).
[66] "Acrylic Recycling For A Cleaner Environment - Polychem USA." https://polychem-usa.com/acrylic-recycling/ (accessed Oct. 16, 2020).
[67] "McMaster-Carr." https://www.mcmaster.com/ (accessed Oct. 16, 2020).
[68] J. R. Taylor and W. Thompson, " An Introduction to Error Analysis: The Study of Uncertainties in Physical Measurements ," *Physics Today*, vol. 51, no. 1. pp. 57–58, 1998, doi: 10.1063/1.882103.
[69] Shenzen PKCELL Battery Co., "SHENZHEN PKCELL BATTERY CO ., LTD Li-Polymer Battery," pp. 3–7, 2014.
[70] F. Semiconductor, "Kinetis K64F Sub-Family Data Sheet," 2015.
[71] "XSENS MTw Awinda," [Online]. Available: https://www.xsens.com/products/mtw-awinda.

APPENDIX A

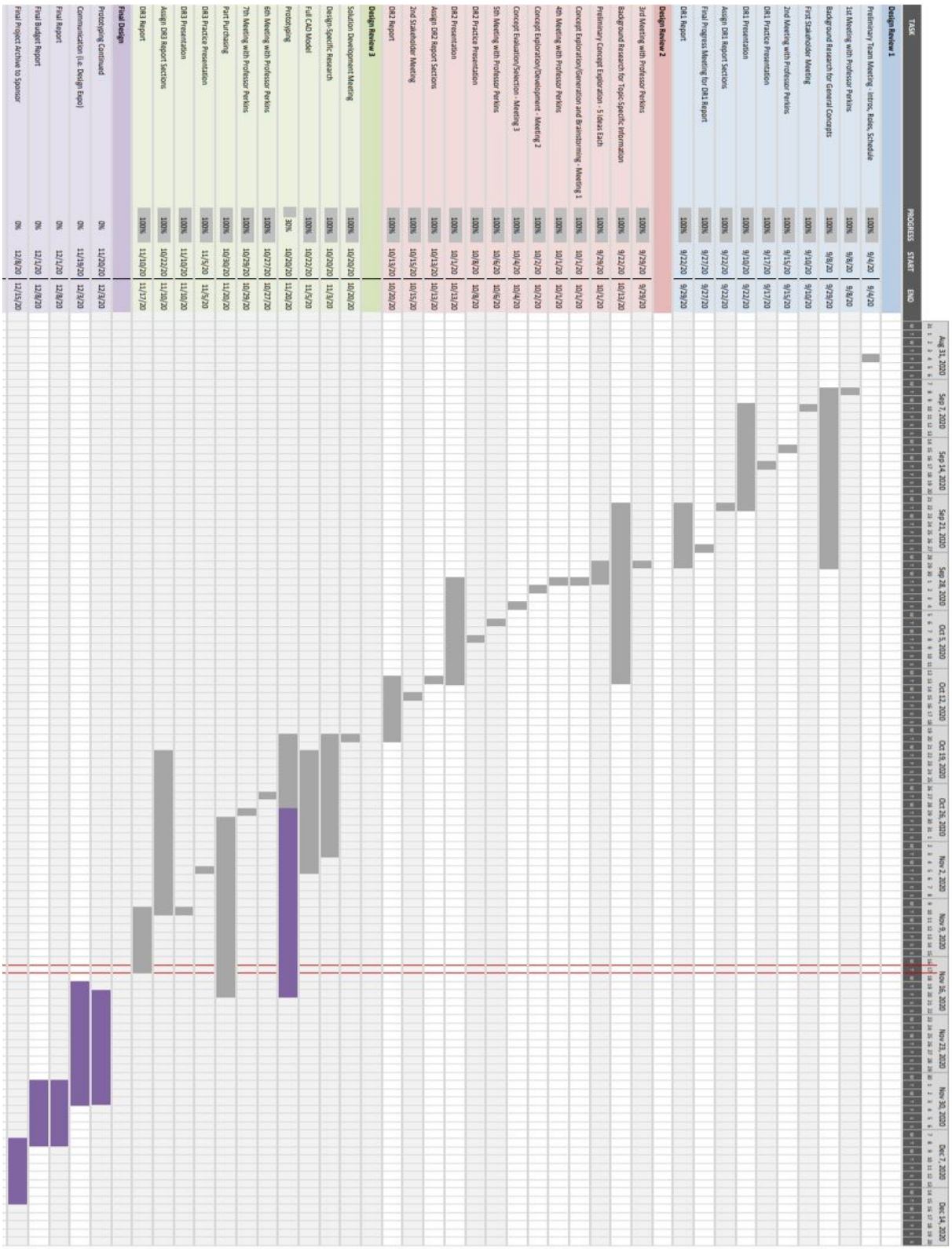

Fig. A.1 Full Gantt chart showing the progress we've made in the report process.

Appendix B

APPENDIX B.1

Concepts generated during concept generation brainstorming session:

The ideas generated for *Consideration 1: Angular Sensor* are as follows:

1. Optical Encoders
2. Hall-Effect Encoders
3. Angular Potentiometers
4. Fiber-Optic Cable Goniometer
5. Protractor (visualization system)
6. Pneumatic pressure sensor
7. Motion capture system
    a. Drones that follow the person
    b. Reflective pattern (LEDs attached to system)
    c. Other visualization
8. Magnetometer and magnet
9. Radioactive element on link and radioactive measurer on the other link
10. Measure inertial force outward
11. Compass trying to find polar north
    a. GPS system on each link
12. Ultrasonic range sensors (echolocation, sonar)
13. Eyeball it
14. IMUs
15. Laser vibrometer
16. Load cell
    a. Torsion spring
17. Heating element and thermometer / thermocouple
    a. Thermo imaging
18. Invent supercomputer to do FEA in real-time
19. X-ray and videoradiography
20. Capacitance change (big plate on the opposite link)
21. Gravitational force between links (put big mass on one side)
22. Neuralink: Feedforward loop for better IMU algorithm prediction

The ideas generated for *Consideration 2: Joint Design* are as follows:

1. Gimbal
2. Rubber band
3. Ball and Socket
4. Literal human arm
5. String / Wire
6. Play dough
7. Bendable links

8. Two individual links
9. Ball bearings
10. Magnet levitation (quantum stuff)
11. Literal magic
12. Compressed gas / water jet adjustments
13. 3-axis gimbal
    a. Camera gimbal off Amazon
14. Hinge
15. Condyloid
16. Fushigi Ball!
17. Bend glue (hot glue)
18. Orbitz
19. Joystick inspiration
    a. One
    b. Two
20. CV Joint
21. Universal Joint
22. Mud
23. Axis-Angle Joint
24. Modeled human shoulder (mechanical bias)
25. Fluidic measurements (accelerations and velocities)

The ideas generated for *Consideration 3: DoF Locking* are as follows:

1. Pins
2. Removeable Gimbal (Modular)
3. Braking System
    a. Clamp
4. Screws
5. Tangle your cords

The ideas generated for *Consideration 4: End-Link Features: Material* are as follows:

1. 3D Printed (PLA)
2. Metals
3. Acrylic
4. Wood
5. Paper (Origami)
6. Wearable (fabrics/textiles)
7. Biomaterials
8. Pretzels

The ideas generated for *Consideration 5: End-Link Features: Portability* are as follows:

1. Telescopable
2. Foldable
3. Nestable
4. Detachable
5. Attachable to drone

6. Attachable to cart
7. Attachable to balloons
8. Rollable

The ideas generated for *Consideration 6: Data Transfer* are as follows:

1. Cable
2. Bluetooth
3. Wi-Fi
4. NFC
5. Magic
6. Flash drive
7. Hard Drive built in
8. Quantum communication (entanglement)
9. Morse Code
10. SD Card
11. Screen display
12. Neuralink
13. Self-Built IMU sensor fusion

The ideas generated for *Consideration 7: Connection Mechanism: Rigid Body* are as follows:

1. Clamp
2. Screws
3. Glue
4. Velcro
5. Double-sided tape
6. Weld
7. Arbor press
8. Pins
9. Ties
    a. String
    b. Zip-ties
10. Epoxy

The ideas generated for *Consideration 8: Connection Mechanism: IMU* are as follows:

1. Machined Slot
2. Machined Corner
    a. Double-Sided Tape
    b. Velcro
    c. Clamp
    d. Glue
    e. Welding
    f. Ties
    g. Epoxy

APPENDIX B.2

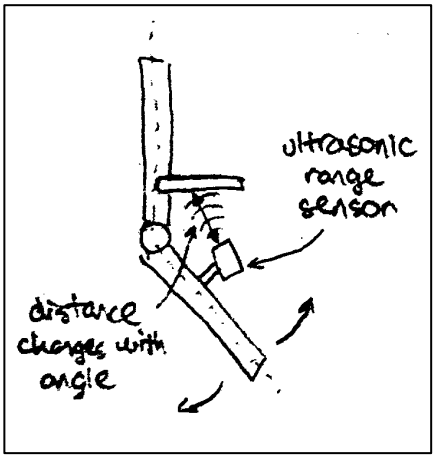

Fig. B.2.1. Angle measurement with range sensor

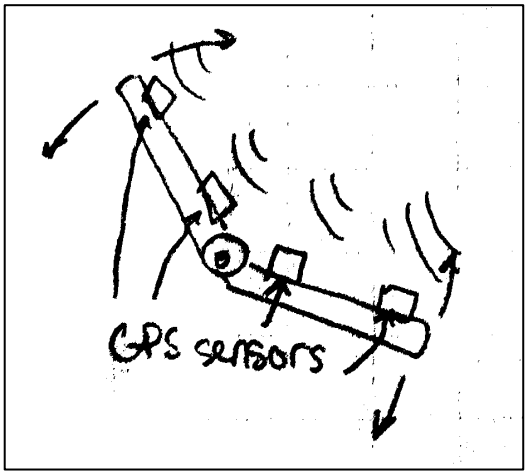

Fig. B.2.2. Using GPS to estimate angles

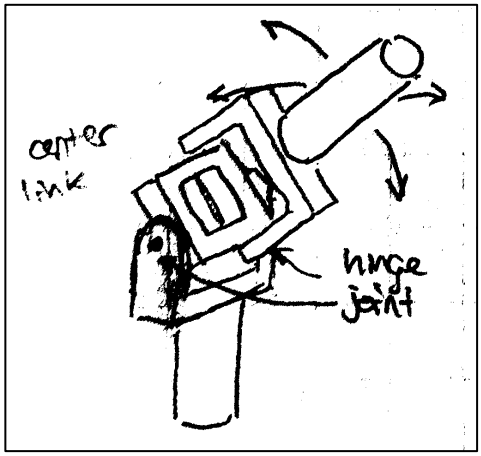

Fig. B.2.3. Universal Joint

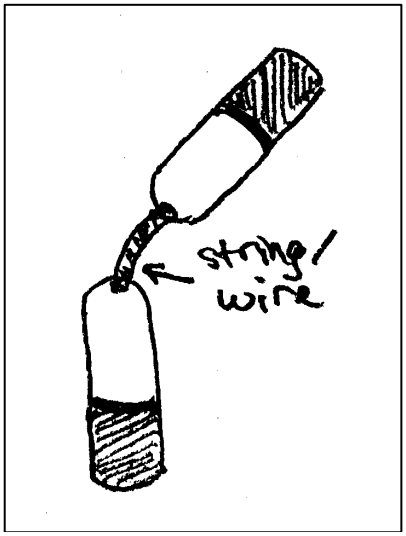

Fig. B.2.4. Join end links with string or wire

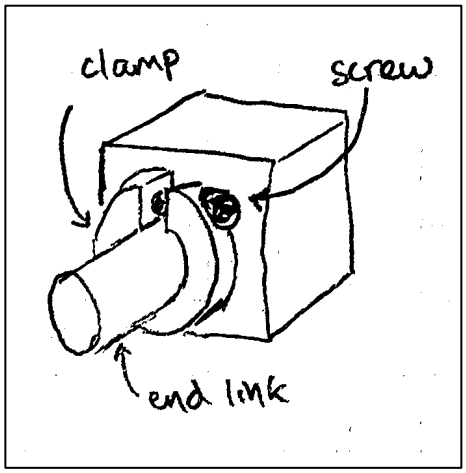

Fig. B.2.5. Clamp design concept

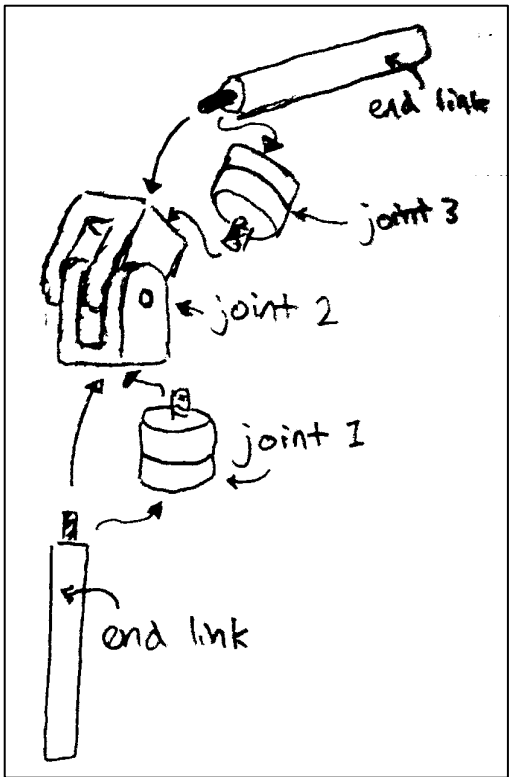

Fig. B.2.6. Modular design concept

APPENDIX B.3

Table B.3.1. Morphological chart showing different outcome options for each category.

Solution Index	Solutions								
	1	2	3	4	5	6	7	8	9
IMU Connection	Machined Datum	Double Sided Tape	Clamp	Screws	Glue	Velcro	Pins	Tape	
Rigid Body Connection	Machined Datum	Double Sided Tape	Clamp	Screws	Glue	Velcro	Pins	Tape	
Degrees of Freedom	Pins	Modular	Braking System						
Actuation	Electric Motor	Pneumatics	Hydraulics	Internal Combustion	Fuel Cell	None			
Portability	Drone	Cart	Foldable						
Data Transfer	Cable	Bluetooth	Wifi	NFC	Flash Drive	SD Card			
End Link Design	Aluminum	3D Print - Plastic	Acrylic	Biomaterials	Stainless Steel				
Joint Design	Gimbal	Rubber Band	Ball and Socket	String/Wire	Playdough/ Bendable Material	Universal Joint	Hinge	Condyloid	CV Joint
Angle Meas.	Optical Encoder	Hall Effect Encoder	Angular Pot.	Fiber-Optic	Strain Gauge/Load Cell	Angular Capacitive Sensor			

APPENDIX C

APPENDIX C.1

There were three key metrics assigned to potential failures: (1) Severity – how large the consequence of the failure mode is, (2) Occurrence – how likely is the failure mode to occur, and (3) Detection – how capable are current design controls of detecting a failure mode. A ranking between 1-5 is assigned for each of these metrics and the product of all three is reported as the final score for any given item. Typical FMEAs call this final output the Risk Priority Number (RPN). The scales for each metric are shown below:

Severity – how large the consequence of the failure mode is

1) No noticeable degradation in performance
2) Fails tier 3 engineering requirement
3) Fails tier 2 engineering requirement
4) Fails tier 1 engineering requirement and or results in loss of data
5) Imposes safety risk to user

Occurrence – how likely is the failure mode to occur

1) Very low (failure is very improbable)
2) Low (relatively few failures)
3) Moderate (occasional failures)
4) High (repeated but predictable failures)
5) Very High (failure all but guaranteed)

Detection - how capable are current design controls of detecting a failure mode

1) Failure always detected
2) Failure detected for majority of occurrences
3) Detect about 50% of occurrences
4) Most failures go undetected
5) Incapable of detecting failures

Table C.1. FMEA - Severity, Occurrence, and Detection are denoted by S, O, and D

Item	Function	Potential Failure Mode	Potential Effects of Failure	Potential Causes of Failure	Current Design Controls	S	O	D	RPN	Recommended Action
Battery	Provide power to sensors and microcontroller	Battery is drained below 3V	May not take charge again and will be useless	Embedded voltage protection circuit and battery charger were damaged	Monitor battery voltage and emit obnoxious warning beep if $V_{bat} < 3V$	4	1	1	4	Replace battery
		Battery is over charged	Could result in small fire		Embedded voltage protection and LED on battery charger	5	2	2	20	
		Battery is dead when you want to collect data	Inefficient and annoying	Battery is always connected to load even when DAQ is not in use	Added E-Stop switch both to disconnect battery when not in use	1	2	1	2	Ensure E-Stop is in off position when not collecting data
Capacitive Angle Sensors	Measure Euler angles	Wiring harness is disconnected	Need to be re-zeroed, loss of data	Wiring harness gets tangled/ snagged	Zip ties used to route wires and provide strain relief	4	2	1	8	Reconnect wiring harness and restart DAQ with push button
		Noise corrupts A and B encoder pulses	Could falsely trigger interrupts used in quadrature decoding	Large amounts of electromagnetic interference	N/A	4	1	1	4	Rework DAQ to include differential line driver output to mitigate noise
SD Card	Stores CSV files containing angle measurements	File is overwritten	Loss of data	SD card capacity reached	Automated file naming prevents MCU from overwriting files when open storage exists	4	2	2	16	Transfer data from SD card to PC regularly

Wiring harness	Transmit data and power to differnt electrical component	broken wire	Need to be re-zeroed, loss of data	Metal fatigue due to exccesive bending/strec hing of the wire	Use multi-thread wiring harnesss	4	1	4	16	Use higer quality wiring harness
3D printed parts	Body of the device	Fragmentation of the device	User unable to use the device	Extensive force or pressure applied	Introducing fillet to reduce pressure concentration	5	1	1	5	Use better 3D printing material or use post processing method such as remelting or anneling
		Cracking and bending of the body parts	Inaccurate reference data collected			4	1	1	4	
	enclose and fix angle encoders					4	1	1	4	
	enclose and fix ball bearings					4	1	1	4	
	Provide reference and mounting datum for IMU					4	1	1	4	
	Provide enclosures for the battery and microcontroller		Less secured circuit board			1	1	1	1	
Ball bearings	Reduce rotational friction, providing better user experience	exccsive wearing	Inaccurate reference data collected	Improper lubrication and maintance	Use pre-lubricated bearings	4	1	1	4	Lubricate and maintance the bearing according to the manufacture
		Jaming due to foreign object	User unable or hard to operat the device	The entering of any foreign objects	Use sealed ball bearings	4	1	1	4	Implement better shielding and improve operating environment
screws	Holding body parts together	stripping or self-untightening	Inaccurate reference data collected	Over tightening or deformation of the 3D printed part	Carefully tighten any screws	1	2	2	4	Modify the design and include more materials for threading; Or use nuts
	Holding encoders in place					1	2	2	4	
	operating DOF locking mechanism					3	2	2	12	

dcoder-shaft coupling	Transmit rotational information from shaft to encoders	stripping or self-untightening of the set screw	Inaccurate reference data collected	Vibration of the shaft	Use threadlocker	4	1	3	12	Use better coupling method or another types of encoder

APPENDIX C.2

High Level Category	Line #	Qty	Unit (ea, pkg, ct)	Item Description	Unit Price	Cost Per Line Item
Electrical/DAQ	1	1	ea	Teensy 3.5 Microcontroller	$ 26.50	$ 26.50
	2	1	ea	1200 mAh LiPo Battery	$ 9.95	$ 9.95
	3	1	ea	Adafruit Micro LiPo Charger	$ 6.95	$ 6.95
	4	2	ea	Adafruit Voltage Booster	$ 3.95	$ 7.90
	5	1	ea	Teensy LiPo Charger	$ 11.95	$ 11.95
	6	1	pkg	Header, Male Pins	$ 4.95	$ 4.95
	7	1	ea	Micro SD: 8 GB UHS-1 Class 10	$ 8.90	$ 8.90
	8	1	ea	SD to USB Reader	$ 7.99	$ 7.99
	9	3	ea	CUI Capacitive Encoders	$ 32.78	$ 98.34
	10	3	ea	CUI Wiring Harnesses	$ 29.07	$ 87.21
	11	1	ea	CUI Programming cable	$ 22.00	$ 22.00
Mechanical	12	6	ea	Ball Bearings	$ 9.40	$ 56.40
	13	1	pkg	Retaining Ring	$ 8.97	$ 8.97
	14	1	ea	3D Printing Filament (PLA?)	$ 20.00	$ 20.00
	15	1	pkg	M3x14 SHCS	$ 11.49	$ 11.49
	16	1	pkg	M3x8 SHCS	$ 7.37	$ 7.37
	17	1	pkg	M3x18 SHCS	$ 11.45	$ 11.45
	18	1	pkg	1/4-20x1.75 SHCS	$ 7.46	$ 7.46
	19	1	pkg	Plastic 3-Arm Knob	$ 1.12	$ 1.12

Total Cost
$ 408.32

Fig. C.2. Bill of materials used for construction of our apparatus showing costs for each component used along with the total cost.

Appendix D

Table. D.1. Detailed Verification Plan. S = Successful, IP = In-Progress, F = Failed

#	Specification	Verification Test	Status
1	Measure Euler angles of links to within ± 1˚	Goniometer measurement	IP
2	Sample at a rate of ≥ 60 Hz	Use timer function to measure code loop rate	S
3	Able to function under torques < 3 Nm	Apply a torque > 3 Nm, and check for structure failure	IP
4	Can move 180˚ along all three axes	Rotate mechanism 180˚ along all three axes, and ensure no locking or hard stops	S
5	> 54 MB of storage	Record data onto SD card until 54 MB is met	S
6.1	Maximum weight of 2 kg	Weigh the mechanism	IP
6.2	Each end link length between 5” and 12”	Measure link lengths with a ruler	S
6.3	Battery-powered for 1 h on one charge	Run battery until it dies or reaches 1 hours	S
7	No materials that change magnetometer reading by > 0.1%	Using a magnetometer measure the unaffected magnetic field, and then the affected magnetic field from the appropriate distance and compare. [a]	IP
8	Can move in 3 degrees of freedom with the capability of locking any of them	Rotate mechanism in all three axis and ensure all three locks work with common forces used in human motion	F
9	Can survive 1200 hours of use	Given the time constraints of the semester, this will not be tested, but it has been designed for	-
10	At least two orthogonal surfaces at attachment sites which locate IMUs within a tolerance of ± 1˚	Measure the angle between the two orthogonal sides and ensure the 1˚ tolerance is met.	IP
11	Data acquired from device to computer in a maximum of 4-6 steps	Count the number of steps needed	S
12	Contains a mechanism able to connect the apparatus to a rigid structure under a force of 8 N in any direction	Apply > 8 N of force in 20 random directions and check for structural failure	IP

Supplemental Appendix

Engineering Standards

For this project, engineering standards were not directly referenced to inform the design. Due to the low physical strains on the design, consideration of standards for design against loading and bearing selection were not necessary. Similarly, due to the low voltages required in the electrical system standards for safety regarding high voltage potentials did not have to be considered.

An engineering standard that did indirectly affect the design of this device was standard voltage potentials in electronics. We had to design around components in the electrical system accepting different standard voltages. The encoders we chose operate on 5V, while the microcontroller accepted only 3.3V. Enabling integration of these devices required the incorporation of a boost converter and voltage-dividing circuitry.

Engineering Inclusivity

Engineering is an incredibly interconnected field. To be responsible, professional, and cognizant engineers, we need to have reasoning behind our decision-making and need to consider the effects that our choices have on people beyond just the immediate stakeholder(s). In our project, we are not designing something that will be used by the general public; it is simply a tool that will be used in Dr. Cain's lab by him and any laboratory staff he has. At first, it might seem a bit challenging on how to consider inclusivity in this context, but in our discussions with Dr. Cain, we've learned that much of his research has to do with studying the biomechanics of people struggling with physical disabilities. So, knowing this, we feel as though helping Dr. Cain is giving us a way to support those with physical disabilities because the more information that can be gathered, the more solutions that can be generated to give people a higher quality of life.

Environmental Context Assessment

The environmental impact of our mechanism played a significant role in our decision making for our design. We wanted to stay conscious of how even a small one-off creation like ours can have a large impact if many others all hold a similar perspective about how a small thing like this won't matter. Thus, we looked into how our mechanism could be designed in an environmentally friendly way, even though the scale is so small. To do this, we created an environmental sustainability weighting for our material selection which led us to use PLA for out end-links. PLA is largely biodegradable when brought to the correct facility, and thus shouldn't have a large environmental impact, although we recognize the odds of it being brought to the correct facility instead of just being thrown in the trash are quite low. However, we also believe that this product will have a relatively large lifetime (at least 1200 hours according to our specification) and thus, for the foreseeable future, it will likely remain in its role as an IMU validation apparatus, which is obviously the best environmental outcome as there will hopefully be no need for replacement parts which take more energy to create and bring about the end-of-life considerations for the previous parts.

We imagine that should the mechanism no longer be needed (or break and not be replaced) the majority of the parts including the sensors, bearings, battery and microcontroller could be easily repurposed for other applications which should also contribute to easing the environmental load of this project.

Social Context Assessment

Social context is highly relevant to this design project. Through supporting research into the joint kinematics of people with physical conditions or injuries, the device we created has the potential to improve the lives of these minority groups. This includes, but is not limited to, Dr. Cain's research subjects. Dr. Cain intends to use our device to validate IMU algorithms that will be used to research the joint kinematics of wheelchair-bound individuals. The development of accurate IMU algorithms will allow him to collect accurate real-world data on subjects without being bound to a laboratory, which will improve the quality of the data he is able to collect on these subjects. Ultimately, this will improve the solutions that are developed to help wheelchair-bound individuals. Because these people stand to gain indirect benefits from our project, we consider them to be secondary, affected stakeholders.

Others in the relevant research space may also be affected by the solution we have developed. We have developed a cost-effective, easily manufactured solution to the problem of IMU joint angle validation. This device could be useful to any researcher looking to develop custom IMU joint angle algorithms for their use case or looking to bring their data collection outside of the lab. These researchers would have direct benefits from our device, and therefore they are primary, affected stakeholders. People who are affected by a physical condition would become secondary, affected stakeholders if the device is adopted for research into their condition.

Ethical Decision Making

As engineers, making ethical decisions is paramount. Engineering fields are at the forefront of technology, so engineers have huge influence into how new technology gets integrated into society. Even though we are just working on a single prototype device for our project, ethical decision making plays a role. We had to consider the safety of the user by designing the joints with no pinch points or sharp edges that could potentially injure the user. Additionally, although we were not experts in the biomechanics field, we feel that, over the course of the project and our mechanical engineering coursework over the past few years, we are competent in this an area of study and can provide valid, useful information and technology. We've strived to make decisions during this project that create positive results for many people and feel like we have been able to accomplish this.